Facilitation drives estrogen receptor positive (ER+) breast cancer growth and survival under drug pressure

Authors:

Rena Emond[1*], Jason I. Griffiths[1*], Vince Kornél Grolmusz[1*], Rachel S. Sousa[2], Andrea H. Bild[1#], Frederick R. Adler[3, 4#]

Affiliations:

[1] Department of Medical Oncology and Therapeutics Research, Beckman Research Institute, City of Hope National Medical Center, Monrovia, CA

[2] Department of Mathematics, Oregon State University, Corvallis, OR, 97331,

[3] School of Biological Sciences, University of Utah, Salt Lake City, UT, 84112

[4] Department of Mathematics, University of Utah, Salt Lake City, UT, 84112

* contributed equally

To whom correspondence should be addressed: Andrea H. Bild (abild@coh.org) and Frederick R. Adler (adler@math.utah.edu)

Abstract

Competition between different lineages of cells within a tumor has been considered in cancer evolution and progression, but positive interactions like facilitation have received far less study. We developed isogenic estrogen positive breast cancer cell lineages (CAMA-1 and MCF7) sensitive and resistant to CDK4/6 inhibition in order to investigate the mechanisms of cell interaction under selective pressure. When these sensitive and resistant lineages are grown in coculture under ribociclib treatment, sensitive cells survive and proliferate better than in monoculture despite the effects of competition. Conditioned media taken from resistant CAMA-1 cells reproduces this advantage, suggesting that secretion of some factor from resistant cells underlies the effect. Liquid chromatography-tandem mass spectrometry (LC-MS/MS) assays were used to identify factors secreted by cell lineages. While the less active estrone metabolite was detected in medium from both lineages, highly active estradiol was only detectable in media that included resistant cells. Because sensitive cells are more dependent on estrogen signaling than resistant cells, they benefit from the increase in local estradiol, leading to facilitated growth when in coculture in the presence of ribociclib. This facilitation of sensitive cells by resistant cells is recapitulated when cells are treated with small molecule inhibitors that target estrogen signaling pathways. We developed a set of mathematical models to quantify the strength of competition and facilitation between cell lines and evaluate the effects of treatments that modify these interactions. These analyses support the conclusion that resistant cell lineages benefit sensitive lineages during therapy through the increased production and sharing of local estradiol, and themselves suffer from increased competition and suppression as a result. Our multidisciplinary approach analyzes and quantifies interactions between ER+ cancer lineages during treatment and provides the framework to evaluate these effects in patients and improve therapy.

Introduction

Almost all tumors are heterogeneous, consisting of cells that differ both genetically and phenotypically (1). This heterogeneity creates three major obstacles for treating cancer. First, cells can have different susceptibilities to treatment, meaning that even a highly targeted and effective treatment might fail to effectively kill or inhibit some cells (2, 3). This differential survival and reproduction is the natural selection that drives the second challenge for treatment, the continued evolution of tumor resistance to treatment (1, 4). For example, many breast cancers are polyclonal at multiple times during their treatment, with evolutionary trajectories showing different subclonal populations responding or resistant to therapy (5). Despite this heterogeneity, current treatment strategies are reactive and directed at treating the resistant state after it occurs instead of developing strategies to prevent its emergence (6, 7). Although several innovative targeted therapies have benefited patient care in a variety of cancers, the selective pressure of these drug treatments favors pre-existing or therapy-adapted cancer cells, which ultimately render the cancer therapy-refractive and lead to disease progression and death. Novel and personalized therapeutic strategies incorporating evolutionary principles show promising results in clinical trials (8).

The third challenge of heterogeneity emerges from ecology rather than evolution (9-14). Heterogeneous cell populations create the possibility for asymmetric interactions among cells that can alter responses to treatment (14, 15). Even in a homogeneous tumor, cells interact through competition for resources and space, and potentially through cooperative interactions such as the production of public goods that recruit resources, suppress the immune response, or poison neighboring healthy cells (16). These interactions provide both targets and challenges for therapy, but have fewer possibilities than asymmetric interactions that could occur among heterogeneous cells, such as those sensitive and resistant to treatment (17, 18). For example, one cell type could aid the other, while suffering from competition itself (19). Such complex cell-cell interactions make predicting response to treatment much more difficult.

As in ecology, competition among cancer cells has characteristic consequences. Most obviously, it reduces overall cell population size because large populations grow more slowly. However, competition also promotes evolution of tumor heterogeneity, because rare types that arise with different needs or limiting factors will have a growth advantage (11, 20). The effects of cell cooperation are more difficult to predict. In general, cooperation helps support larger populations (21). Evolutionary ecologists have demonstrated that switching from competition to cooperation can promote coexistence of populations with higher densities when cooperators co-occur (22, 23). A combination of positive and negative interactions can promote greater persistence and growth than in simpler systems with resource competition alone (24). Interactions that change from beneficial at low density to competitive at high density can create more persistent communities (25). Cooperation can act to increase or reduce diversity depending on the specific mechanisms involved (26-28). Of most concern, cooperation may enhance the potential for tumors to be resistant to treatment if cells work together to combat the new challenge (21, 29).

Cooperation takes on multiple types, and almost never exists in isolation from competition (30, 31). Competitors can benefit each other through defense against threats or enhanced access to resources. We use the term **facilitation** to describe cases where competitors of one species benefit those of another (32). For example, among plants competing for water, one can see facilitation when one individual gains from water that leaks from the roots of a deeper-rooted neighbor (33) This coincidence of competitive and facilitative interactions requires detailed mathematical models to disentangle their concurrent effects, and manipulative experiments to identify specific modes of competition and cooperation.

When does cooperation arise? Evolutionary ecologists have defined many factors that promote its evolution and maintenance (26, 34-36). The role of environmental stress, the stress gradient hypothesis (25), is of particular relevance to cancer. Spatially explicit models indicate that cooperation is more likely to persist in regions of high stress, such as cells undergoing drug treatment, where cooperative benefits outweigh the competition for resources (37). Furthermore, clonal cooperation can occur and be maintained through many interactions such as cell-cell physical communication and paracrine effects (38). As cell proliferation is regulated by signaling, nutrient availability, growth factors, and other means, increasing growth factor abundance and activating pro-proliferative signaling pathways during cooperation can contribute to tumor growth (21). Differential production of certain factors amongst heterogenous subclones, such as increased FGF2 in afatinib resistant lung cancer cells, has been linked to acquisition of resistance (39). Additionally, polyclonal breast tumors comprised of various subclones, two of which expressed increased IL-11 and FIGF were shown to drive tumor growth and polyclonal metastasis through clonal cooperation (40).

This study addresses cell interactions in breast cancer. This common cancer is classified into three main subtypes with hormone receptor-positive tumors, including estrogen and progesterone receptors, making up 75% of cases (41). Tumors are known to be polyclonal at multiple times during their treatment, with evolutionary trajectories showing distinct populations responding or resistant to therapy (5). Yet, the extent of cooperation and competition among these populations remains unknown. Interestingly, endocrine therapy is given as primary treatment, even if a patient's tumor shows just 1% estrogen receptor (ER) expression, as these patients often respond despite the heterogeneity (42). This exemplifies the interconnectedness of tumor populations and although the underlying cause of response remains incompletely understood, the breakdown of cooperative cell interactions within a heterogeneous tumor is a possible cause (26).

Endocrine therapies are estrogen antagonists that either deplete estrogen made endogenously or by breast cancer cells (aromatase-inhibition) or block ER activity through modulation or degradation (5, 43, 44). At least 33% of patients with early-stage disease will develop endocrine resistance, increasing to approximately 90% of patients with metastatic disease (45, 46). Combination of endocrine therapy with cyclin-dependent kinase (CDK) 4/6 inhibitors of the cell cycle has improved disease control in metastatic ER+ breast cancer. To determine efficacy in additional patient populations, adjuvant trials are underway to study the efficacy of this combination in early stage, non-metastatic breast cancer (47-52). Preliminary results after short term follow-up from adjuvant trials have shown contradictory results, with the MonarchE trial showing an improvement in invasive disease free survival with two years of adjuvant abemaciclib added to endocrine therapy, the PALLAS trial failing to show an improvement in

the same endpoint after two years of adjuvant palbociclib (49, 52) and the FELINE trial showing no improvement in cell cycle arrest after 6 months of therapy (53).

We have developed isogenic ER+ breast cancer cell lineages sensitive and resistant to CDK4/6 cell cycle inhibition (54) and use lines derived from two cell lines, CAMA-1 and MCF7, to investigate cooperative and competitive cell interactions in heterogeneous cancer populations during selective pressure and probe for differences in growth, resistance, and interaction between cell types. Our experiments test how these cells respond to the CDK4/6 inhibitor, ribociclib, in both monoculture and coculture. Based on our finding that resistant cells facilitate growth of sensitive cells under CDK4/6 inhibitor treatment, we challenged the system with estradiol and a set of ER antagonists to investigate the mechanisms underlying this facilitation.

We use mathematical models to quantify the strength of interactions and their underlying mechanisms. The experiments take two general forms. To test the interaction of ribociclib treatment with cell-cell interactions, and with other treatments, we measure growth in a fully factorial design with treatment either on or off and cells grown in monoculture and coculture, and fit the growth curves with logistic and Lotka-Volterra models. To accurately quantify the key differences between sensitive and resistant cells, we conducted a separate set of challenges to monocultures and cocultures of sensitive and resistant cells with a range of ribociclib doses and estimate the parameters of a detailed mechanistic model. This consumer resource model describes the asymmetric facilitation of sensitive by resistant cells, and is used to quantify the key differences between sensitive and resistant cells, reveal how facilitation impacts heterogeneous cancer population growth during treatment, and indicate how facilitation modification could be used to jointly control resistant and sensitive population.

We combine these experiments and models to address the following questions:

1. Do sensitive and resistant cells compete symmetrically, or does resistance lead to lower competitive ability?
2. What signals from resistant cells mediate the facilitation of sensitive cells under CDK4/6 treatment?
3. If estrogen signaling plays a central role, how do cells respond to manipulation through direct addition of estradiol or ER antagonists?

Results

Sensitive and resistant cell growth and treatment effects

We used an in vitro model to study ER+ breast cancer cell interactions under selective drug pressure. Ribociclib resistant lines were evolved under continuous exposure to treatment, and with acquired resistance confirmed by dose-response experiments. We labeled parental sensitive cells (venus label green) and ribociclib resistant cells (either cerulean blue in CAMA-1 cells or mcherry red in MCF7 cells) with distinct fluorescent proteins. In order to quantify growth rates and better understand the degree of therapy resistance between ribociclib resistant and sensitive cell lines, experiments with 3D monoculture spheroids were performed under different conditions (without treatment or with ribociclib treatment of varied dose concentrations). To

quantify growth under these conditions, we measured fluorescence intensity and growth of spheroid area over an 18-day period (days 0, 4, 7, 11, 14, 18).

In monoculture, sensitive CAMA-1 cells grew more quickly than resistant cells, while under ribociclib therapy at both 200nM and 400nM drug concentrations, resistant cells grew more quickly than sensitive **(Fig. 1a).** Proliferation of sensitive cells decreased under ribociclib treatment (and to a greater degree with increased drug concentration), whereas resistant cells had a less dramatic change in proliferation rate with treatment. The statistical interaction between cell type (sensitive and resistant) and treatment is highly significant, showing that sensitive cells grow more quickly than resistant cells in the absence, and more slowly in the presence, of ribociclib treatment **(Fig. 1b)**.

In a second ER+ breast cancer line, MCF7 **(Fig. 1c)**, the resistant cell population grew more quickly than sensitive cells, even without therapy, indicating the lack of an often-assumed cost of resistance. However, resistant cells continued to grow under therapy although at lower rates at higher doses, while even the lowest dose effectively halts the growth of sensitive cells **(Fig. 1d)**. Despite these differences in the untreated setting, resistant cells in both cell lines show a greater ability to tolerate treatment.

<u>Ribociclib therapy induces facilitation of sensitive cells by resistant cells</u>

To investigate whether cell interactions alter response to therapy, we cocultured sensitive and resistance cells under different treatments over time. For CAMA-1 cells, we plated spheroids at different compositions (100% sensitive monoculture, 50% sensitive – 50% resistant coculture, 100% resistant monoculture) and observed proliferation for 18 days with or without treatment. To visualize, the 50%-50% mixed coculture image is split by fluorescence to separate sensitive and resistant cell populations within the mixed spheroid. MCF7 spheroid experiments were performed similarly but to adjust for the higher growth rate of resistant cells, we plated cocultures at 90% sensitive-10% resistant. We compared each population's growth in treated coculture with the expected population trajectories from a Lotka-Volterra competition model, based on growth parameters estimated in monoculture without and without treatment, and their competitive ability estimated from growth in untreated coculture. We use the mathematical model to predict spheroid growth if the strength of cell-cell interactions does not depend on treatment. Specifically, we multiplicatively combined the effect of treatment on monocultured sensitive and resistant cells with the effect of coculture without treatment to predict growth in treated coculture (see Methods for details). Deviations of cocultured resistant or sensitive cell growth curves from this null model expectation indicates a more complex cell-cell interaction **(Fig. 2a**), and growth more rapid than predicted in coculture indicates facilitation.

With CAMA-1 cells, ribociclib drug treatment of 200nM and 400nM concentrations inhibits growth of sensitive cells more than resistant cells in monoculture (**Fig. 2b**), consistent with results in **Fig 1**. However, sensitive cells proliferated better when cocultured with resistant cells. The excess of sensitive cells in coculture at the conclusion of growth occurs despite the smaller initial number of sensitive cells in coculture due to plating at half the cell concentration of the monoculture to achieve a 50%-50% population.

Using mathematical models, we find that sensitive cells strongly suppress resistant cells in untreated CAMA-1 cocultures, with a competitive effect 50% larger than that of resistant cells on themselves. In contrast, resistant cells have almost no detectable competitive effect on sensitive cells (**Fig. 2c**). In ribociclib treated coculture, the null model predicts that sensitive cells will grow slightly more slowly than in treated monoculture due to competition, but we find instead markedly increased growth showing facilitation of sensitive cells by resistant cells (**Fig. 2d**). Reciprocally, resistant cells grow more slowly than expected in treated coculture, due to the increased suppression by the sensitive cells they facilitate.

In MCF7 cells, sensitive monoculture growth was inhibited under 1.5uM or 2.4 uM ribociclib drug treatment, while resistant cells displayed higher drug tolerance and better survival **(Fig. 2e)**. MCF7 cells thus show resistance despite a lack of measurable costs in monoculture, a result that carries over to coculture experiments where we see no evidence of competitive asymmetry (**Fig. 2f**). Despite these differences in the innate resistance and its costliness between lineages, the same pattern of facilitation emerges; although with smaller magnitude, sensitive cells benefit from the presence of resistant cells and resistant cells grow more slowly due to increased competition at the highest treatment dose (**Fig. 2g**).

Mechanisms of facilitation under ribociclib treatment

To determine the mechanisms driving facilitation during ribociclib treatment, we conducted a series of additional experiments on CAMA-1 cells. First, we tested whether resistant cells metabolize ribociclib more effectively than sensitive cells, resulting in a lower ribociclib concentration and allowing increased proliferation of cocultured sensitive cells. Using an optimized HPLC/MS method, we found that the ribociclib concentration was not decreased in media incubated with resistant spheroids more than with sensitive spheroids and remained at high doses (results not shown).

Alternatively, ribociclib resistant cells may release signaling molecules that enhance the growth of sensitive cells under drug treatment. To test this hypothesis, we compared proliferation of sensitive cells when supplemented with conditioned media transferred from spheroids of different compositions (100% sensitive, 50%-50% sensitive/resistant, 100% resistant) with or without treatment (0 or 400nM ribociclib). Conditioned media originating from spheroids of resistant cells increased proliferation of sensitive cells more than conditioned media produced by spheroids containing only sensitive cells, with the largest difference when the cells providing the media were themselves treated **(Fig. 3a)**. This increased growth of sensitive cells provides evidence that resistant cells secrete signaling molecules that provide pro-growth benefits for sensitive cells under drug pressure.

To identify the molecules secreted by resistant cells and responsible for promotion of sensitive cell growth under drug pressure, we measured concentrations of several hypothesized factors in the media of cultured spheroids We used liquid chromatography-tandem mass spectrometry (LC-MS/MS) assay to detect estrone (Supplemental Figure 1) and estradiol concentration under no treatment or 400nM ribociclib treatment **(Fig. 3b)**. Estradiol was not detectable in media from 100% sensitive cell cultures in either treatment while samples from cultures containing resistant

cells showed measurable levels. By fitting a model of production and uptake by cells as corrected for cell number and limits of detection, we estimate that resistant cells produce approximately 8 times more estradiol and use 2.5 times more estradiol than sensitive cells **(Fig. 3c)**. Custom multiplex cytokine analysis for detection of other growth factors of interest (TGFβ 1-3, TGFα, EGF, and FGF2, 21, 23) showed no significant differences between untreated and ribociclib treated conditions of the monoculture or coculture of sensitive and resistant cells, further supporting estradiol secretion by resistant cells as a leading mechanism promoting growth of sensitive cells in coculture under ribociclib (Supplemental Figure 1).

We investigated this proposed mechanism by adding estradiol or one of three ER antagonists (fulvestrant, tamoxifen, and raloxifene) to the medium and assessing growth in monoculture **(Fig. 3d)**. Estradiol increased growth of sensitive cells and decreased that of resistant cells. Each of the three ER antagonists reduced the growth of both sensitive and resistant cells, but with different relative effects. Fulvestrant and tamoxifen reduced growth of sensitive cells by less than that of sensitive cells, while raloxifene produced no significant difference. This indicates that sensitive cells depend strongly on the ER pathway for growth, with more specific effects in resistant cells.

To test whether proposed mechanisms lead to drug synergy, we treated monocultures of sensitive and resistant cells with combination therapy of ribociclib and one of the estrogen pathway modifiers. We developed a null model of our expectation for monoculture growth without facilitation, multiplicatively incorporating the effects of the two treatments (see Methods). Sensitive cell monocultures grew more than expected under combination ribociclib and estradiol therapy, replicating the effect of facilitation in coculture, while resistant cells showed no significant deviation. When pooled, the three ER antagonists show a synergistic interaction with ribociclib, reducing the growth of both cell types more than expected, and more strongly impacting sensitive than resistant cells **(Fig. 3e)**. Despite the distinctive responses of the two cell types to the three ER antagonists individually, we find consistent synergistic responses in both sensitive and resistant cells **(Fig. 3f)**.

Modifying the endocrine signaling pathway affects facilitation

Applying ribociclib treatment in coculture revealed facilitation of sensitive cells by resistant cells and treating monocultures with estrogen pathway modifiers indicates that excess estradiol production by resistant cells activates pathways in sensitive cells that can partially evade the effects of treatment. To complete the picture, we test the effects of estrogen pathway modifiers on cells in coculture, both with and without ribociclib treatment.

Across all modifier spheroid experiments (**Fig. 4a-4d**), sensitive cell proliferation was enhanced when cocultured with resistant cells compared to growth in monoculture, supporting previous findings of facilitation. To determine the generality of facilitation, we tested whether coculture alters growth in the presence of each modifier (estradiol and ER antagonists) without ribociclib. Estradiol treatment alone has a smaller beneficial effect on sensitive cells in coculture than predicted under a null model, consistent with the redundant effects of coculture and estradiol in stimulating sensitive cell growth (**Fig. 4a**). Resistant cells are facilitated by sensitive cells when

treated with estradiol, perhaps because sensitive cells reduce concentrations of a hormone that is detrimental to resistant cell growth. With ER antagonists, sensitive cells are in general facilitated by resistant cells, most strongly with fulvestrant, more weakly with raloxifene, and with no significant effect with tamoxifen (**Fig. 4e)**.

Finally, after assessing each modifier alone, we ask whether estrogen pathway modifiers interfere with the facilitation of sensitive cells by resistant cells in our spheroid experiments when treated with ribociclib, which we term facilitation modification. Combining estradiol with ribociclib resulted in similar growth dynamics in the sensitive cells both in monoculture and coculture, with little effect on the strength of facilitation (**Fig. 4a**). When ribociclib was combined with ER antagonists, facilitation of sensitive spheroid growth was generally increased, least of all with tamoxifen (**Fig. 4b)** but more strongly with fulvestrant (**Fig. 4c)** and raloxifene (**Fig. 4d**). To precisely quantify these effects, we compare observed growth with a null model that assumes no facilitation modification. For sensitive cells, we observe little facilitation modification by estradiol and a relatively weak effect of tamoxifen. With fulvestrant and to a lesser extent raloxifene, we see stronger facilitation modification than expected, consistent with the fact that resistant cells facilitate sensitive cell growth to both ribociclib and these two ER antagonists (**Fig. 4f**).

Identifying and measuring the role of facilitation

The experiments using a small number of doses of ribociclib quantify the strength of resistance and facilitation and can be combined with a single dose of each estrogen modifier to reveal the broad structure of interactions. However, establishing the underlying mechanisms requires data with more levels of ribociclib. We measured growth of sensitive and resistant cells with five doses of ribociclib and compared fits of several more detailed mechanistic models that treat cell growth and death separately and include specific functional forms for the effects of ribociclib and estradiol **(Fig. 5a)**.

The detailed model of the mechanism of facilitation accurately describes the growth of resistant, sensitive and coculture spheroids under a broad range of drug doses **(Fig. 5b)**. The fitted facilitation model also quantifies how biological processes differ between resistant and sensitive cells **(Fig. 5c)**. Resistant cells are approximately 60% as competitive, consistent with the 1.5 times higher competitive effect of sensitive cells (**Fig. 2b**). Because we did not measure estradiol directly, we cannot separately identify the parameters associated with production and uptake, and instead an overall production of facilitation factor by resistant cells was measured which is approximately twice that of sensitive cells, again consistent with the ratio of production/use estimated directly (8.0/2.5 = 3.2, **Fig. 2c**) . In the absence of treatment, the less competitive resistant cells had a lower baseline division rate (50% that of sensitive cells) and a lower quiescence rate. However, they were far less sensitive to the cell cycle inhibitory effects of ribociclib, allowing their spheroids to continue to grow at high doses.

Next, we compared alternative hypotheses about the processes generating the observed spheroid growth trajectories to verify that the facilitation hypothesis was well supported by the data **(Fig. 5d)**. Based on formal model comparison, using Watanabe–Akaike information criterion (WAIC)

to penalize for the complexity of our Bayesian models, we found that models incorporating facilitation greatly outperformed (lower penalized prediction error) models of competition alone and models of phenotypic plasticity, either through drug induced (DI) or random switching (RS) of phenotypic states (see Methods). Furthermore, facilitation models in which resistant cells contribute disproportionately to the production of facilitation factors (asymmetric facilitation) greatly outperformed simpler facilitation models assuming equivalent facilitation by resistant and sensitive cells (symmetric facilitation). Describing the cell cycle inhibitory mechanism of action of ribociclib through the addition of quiescent and senescent cell states further improved model accuracy compared to simpler models in which ribociclib simply reduces cell division rates. These additional states allow prediction of the delayed impacts of therapy at higher doses (reducing penalized prediction error) and also estimation of the rate of division and quiescence with and without therapy.

We used the fitted model to predict the impact of therapeutically blocking facilitation on the growth of sensitive and resistant cell coculture populations. In the model, the binding of the facilitation factor to its specific cellular receptor was reduced by differing degrees, reflecting exposure to different doses of a receptor blocking drug such as Fulvestrant. In the absence of facilitation blocking, the facilitation model accurately predicts the final resistant and sensitive cell population size (**Fig. 5e**; points show observed final cell counts at day 21, black line shows model predictions). Blocking facilitation factor binding was predicted to reduce the final resistant and sensitive cell population sizes across all ribociclib doses. However, facilitation needed to be reduced by more than 50% before substantial reductions in spheroid growth were predicted. This suggests that sufficiently large amounts of facilitation factors were produced to saturate the growth benefits of facilitation and that a large fraction of this signal must be inhibited for facilitation blocking to be effective. At lower ribociclib doses (<500nM), facilitation blocking caused a more severe reduction in the abundance of sensitive than resistant cells. The greater susceptibility of sensitive cells likely reflects the ability of the resistant cells to pre-empt the facilitation factor. This is consistent with the small observed growth benefit resistant cells experience under combination treatment with ribociclib and estradiol (**Fig. 3f**).

Finally, we assessed the importance of facilitation relative to competition in determining the rate of spheroid growth throughout treatment **(Fig. 5f)**. Across a broad range of ribociclib doses (<600nM) we identified a window of time during spheroid growth when facilitation was many times more important than competition. This period followed the accumulation of a sufficient population size to generate high levels of facilitation factors but ends prior to the spheroid reaching its maximal density and becoming regulated by resource limitation. At moderate ribociclib doses (200-600nM), the facilitation window shifts later into the treatment, as cell abundances increase more slowly, and the window also extends for a longer duration. At the highest ribociclib doses (>600nM), the window of facilitation closes completely. At these doses the coculture spheroid shrinks during treatment, preventing the growth of a population sufficient to produce enough facilitation factor to overcome treatment.

Discussion

We developed in vitro model systems to investigate whether and how clonal cooperation impacts the growth of heterogeneous estrogen positive breast cancer populations. Using cells resistant and sensitive to ribociclib (CDK 4/6 cell cycle inhibitor), we compared population growth in monoculture and in coculture and against different treatment backgrounds, and used mathematical models to unravel the contributions of treatment effects, competition, and cooperation. In both the CAMA-1 and MCF7 lineages, cells adapted to be resistant were indeed able to grow better under treatment (**Fig. 1**), although only CAMA-1 cells showed a cost of resistance in the absence of therapy. Consistent with this result, sensitive CAMA-1 cells strongly suppressed resistant cells in untreated coculture, with little reciprocal competitive effect (**Fig. 2c**). In contrast, competition was symmetric in MCF7 cells (**Fig. 2f**). Despite these competitive and fitness differences, both cell lines showed facilitation of sensitive by resistant cells when treated with ribociclib when cocultured (**Fig. 2b,d,e,g**).

After showing that the facilitation was not due to increased uptake of ribociclib by resistant cells, we reproduced facilitation by adding media from resistant cells (**Fig. 3a**), implying that some secreted factor mediates facilitation. We hypothesized that this factor would be related to growth and could be a growth factor that activates receptors that drive proliferation or estradiol that triggers the estrogen signaling that plays a key role in ER+ cancer cell growth. Increased levels of estradiol or growth factors may also serve to bypass resistance mechanisms found in ER+ breast cancer, such as downregulation or mutation of ER (53, 55). This work provides several lines of evidence that support the role of estradiol in facilitative growth. First, resistant cells produce approximately 8 times more estradiol than sensitive cells (**Fig. 3c**). Our studies did not show a significant difference in levels of secreted growth factors between resistant and sensitive cells. Estradiol also has no effect on resistant cells under ribociclib treatment, consistent with their general indifference to supplementation of a hormone that they readily produce. Second, adding estradiol recapitulates the facilitative effect on sensitive cells, providing partial resistance to ribociclib (**Fig. 3e, f**). With estradiol treatment of cocultured spheroids, sensitive cells receive no additional growth boost from resistant cells, perhaps because the signals have redundant effects on cell cycle progression. Three ER antagonists (fulvestrant, tamoxifen, and raloxifene), in contrast, enhance the effect of ribociclib in both cell types, and more so in sensitive cells (**Fig. 3e,f**), consistent with their complementary effects on blocking ER+ cancer cell growth driven by activation of ER and subsequent CDK4/6 cell cycle proteins. This drug synergy is consistent with the clinical effect of the combination in patients, which shows remarkable efficacy in metastatic ER+ breast cancer (56, 57). As our third line of evidence, resistant cells also facilitate sensitive cells when treated with ER antagonists in coculture, perhaps due to overcoming the antagonism with additional estradiol as with ribociclib treatment (**Fig. 4e**).

Using our understanding of the mechanism of facilitation, we constructed a detailed consumer-resource model to estimate from the population growth curves the strength of cell interactions, vital rates of cell proliferation, quiescence and senescence and the differential susceptibility of sensitive and resistant cells to treatment (**Fig. 5a-c**). This dynamical model can be used to quantify the role of facilitation in supporting heterogeneous cell populations as mass increases and in response to differing drug concentrations. We found that facilitation of sensitive cells

supports the continued growth of heterogeneous cancer cell populations during therapy intermediate doses of cell cycle inhibition (**Fig. 5b**). Accounting for the mechanism of facilitation allowed us to accurately explain spheroid growth trajectories across cell compositions and drug dosing treatments. In contrast, other cell mechanisms such as competition alone between cells and drug induced or drug independent phenotypic switching did not match the sensitive cell population growth (**Fig. 5c**). Specifically, we found strong evidence that facilitation signals are asymmetrically provided by resistant cells (**Fig. 5d**). In coculture, this allowed an increase in sensitive cell abundance relative to monoculture at drug doses in the nanomolar range. A key finding is that blocking facilitation has the potential to control both resistant and sensitive cell populations and inhibit the development of a sole refractory population (**Fig. 5e**).

This model highlights that the contribution of facilitation to proliferation and cancer population growth is not constant but shifts during the growth of the cancer. As cell abundance increases, facilitation-driven growth diminishes as carrying capacity is reached, due to an increase in resource competition (**Fig. 5f**). This suggests that competitive ability may be more essential at later stages in disease progression, while cooperation may be more important in earlier stages. Facilitation is also expected to be ineffective at low population sizes, when cells cannot produce sufficient concentrations of facilitation factor. With these Allee effects, cancer populations below a critical abundance cannot generate enough proliferative signals to grow despite the effects of treatment, leading to further reduced facilitation and the population being driven to eradication. Within patient tumors, other regulatory mechanisms may cause more complex forms of frequency or density dependent growth. Nevertheless, blocking facilitation has clinically valuable features that deserve additional assessment.

Several observations require further investigation. In CAMA-1 cells, we do not understand the mechanisms underlying the negative effects of estradiol on resistant cells despite their higher production and uptake. Although estradiol could underlie the asymmetric competitive effects of sensitive cells, we need to conduct further investigation to uncover the full mechanism. In addition, we do not yet have the experimental resolution to explain whether the differences in effects of the three ER antagonists, such as the much stronger effects of fulvestrant, are due to differences in dose or mechanism of action. In MCF7 cells, we see no evidence for costs of resistance, and no asymmetry in competitive effects, and need to investigate these mechanisms under a wider range of conditions.

Our study has several limitations. First, the work is done in cell culture, and thus cannot account for the many additional factors and interactions that occur in a real tissue. Second, we investigate only two cell lines, and have not shown that the mechanism of facilitation through estradiol operates more generally, including in cells taken from patients. Third, we investigate only a single dose of each estrogen pathway modifier, and thus cannot yet calibrate their effects over a full range.

Mathematical modeling (58-60) and experimental (27, 61, 62) research proposes that tumor growth and progression may be promoted by cooperation between cells by sharing of resources or by-products in diverse cell populations. Some examples include neoangiogenesis to supply nutrients and oxygen and growth factor production to drive proliferation. Together, our results support the concept that cancer cell facilitation may impact heterogeneous tumor growth during

treatment. No current therapy is directed specifically at cancer cell interactions. However, as tumors are often comprised of multiple different subclonal populations, interactions between cells and their impact on the effectiveness of therapy may provide targets for long-term treatment strategies. Indeed, the experiments detailed above highlight how drug resistant cells enable normally sensitive cells to survive during standard of care treatments. In some cases, these sensitive cells may show increased proliferation due to the potential fitness costs of resistant cells, which we see here in CAMA-1 but not MCF7 lineages. As we gain in capabilities to measure the growth of heterogeneous subclone populations during treatment, we may tailor strategies to control faster growing yet drug sensitive cells while preventing dominance of refractory cells through competition with more fit subclones.

This study is the first to describe facilitation through an increase of local estradiol concentrations by resistant cells, which stimulates proliferation of sensitive cells during selective pressure due to higher dependence on and response to estrogen. It is known that estrogen biosynthesis and metabolism can occur in cancer cells (63-65). It remains unknown how resistant cells in our system acquire the ability to modulate estradiol levels. However, the increase of this active estrogen is important given that the majority of breast cancers are hormone receptor positive, and resistance to first line standard of care hormone therapy is common (66-68). In patients with increased levels of local estradiol, potential treatment strategies could include blocking enzymes that synthesize estradiol in resistant cells or modulating the level or type of endocrine therapy given to a patient. As multiple options for treatment timing and dosing exist, as well as many different tumor compositions, modeling these data will help focus on approaches with most potential for experimental testing.

In conclusion, our data indicate that the interactions within heterogeneous cancer cell populations shape the dynamics of resistance and cancer growth of the population as a whole. We show that local production of a highly active estrogen, estradiol, facilitates the growth of sensitive cells, is produced by resistant cells, and conveys resistance to anti-proliferative effects of cell cycle inhibition in sensitive cells. We use mathematical models to show that blocking this facilitation mechanism promotes response of the entire cancer population, reducing selection for refractory resistant states. This work provides support for the development of novel cancer therapeutics that include consideration of cooperation in breast cancer.

Methods

Lentiviral labeling of sensitive and resistant cells

Lentiviruses incorporating Venus (LeGO-V2), mCherry (LeGO-C2), and Cerulean (LeGO-Cer2) fluorescent proteins were generated using Lipofectamine 3000 reagent (Thermo Fisher Scientific) according to the manufacturer's instructions. LeGO-V2, LeGO-C2, and LeGO-Cer2 vectors were gifts from Boris Fehse (Addgene plasmids #27340, #27339, and #27338) (69). MCF7 and MCF7_ribociclib_resistant cell lines were transduced with Venus- and mCherry-containing lentivirus, respectively using reverse transduction, resulting in MCF7_V2 and MCF7_riboR_C2 cell lines. CAMA-1 and CAMA-1_ribociclib_resistant cell lines were

transduced with Venus- and Cerulean-containing lentivirus, respectively using reverse transduction, resulting in CAMA-1_V2 and CAMA-1_riboR_C2 cell lines. Briefly, 1 ml of polybrene-containing cell suspension of 200,000 cells were plated in a well of a 6-well plate, where 0.5 ml of viral aliquot was previously dispensed. Cells were incubated for 48 h at 37 °C and 5% CO2, after which cells were washed and fresh regular culture medium was applied. Fluorescently labeled cells were selected using fluorescence-activated cell sorting after further subculture of transduced cells to attain homogeneously labeled cell populations and used for 3D spheroid experiments.

Cell lines and reagents

The previously authenticated estrogen-receptor-positive (ER+) CAMA-1 and MCF7 breast cancer cell lines were maintained in DMEM+ 10% FBS+ 1% antibiotic–antimycotic solution. . CAMA-1 cells were continuously treated with ribociclib (Selleck Chemicals, Cat. No: S7440) at 1 µM concentration for 1 month followed by 250 nM for 4 months to develop resistance. Ribociclib-resistant CAMA-1 cells were further maintained in complete culture medium supplemented with 250 nM ribociclib. MCF7 cells were continuously treated with ribociclib at 5 µM concentration for 1 month followed by 1.5 µM for 4 months to develop resistance. Ribociclib-resistant MCF7 cells were further maintained in complete culture medium supplemented with 1.5 µM ribociclib. Resistance was detected by the alteration of the dose–response curve measured using CellTiterGlo Chemoluminescent Kit (Promega Corporation, Cat. No.: G7573).

Mono- and coculture 3D spheroid experiments

For CAMA-1 spheroid experiments, 2000 cells were plated in different proportions (100% CAMA-1_V2, 50% CAMA-1_V2—50% CAMA-1_riboR_Cer2, 100% CAMA-1_riboR_Cer2) in 96-well round-bottom ultra-low attachment spheroid microplate (Corning, Cat. No.: 4520). For MCF7 spheroid experiments, 5000 cells were plated in different proportions MCF7: 100% MCF7_V2, 90% MCF7_V2—10% MCF7_riboR_C2, 100% MCF7_riboR_C2) in the same 96 well microplate. 24 h later, spheroids were washed and fresh medium including treatment drugs was applied. Spheroids were treated for a total of 18-21 days with imaging and media change performed at every 4th and 7th day of the week. Spheroids were treated with the following drug therapies at specified doses described in results: ribociclib (Selleck Chemicals, Cat. No: S7440), estradiol (Peprotech, Cat. No: 5022822), fulvestrant (Selleck Chemicals, Cat. No: S1191), tamoxifen (Selleck Chemicals, Cat. No: S7827), and raloxifene (Selleck Chemicals, Cat. No: S5781). Imaging was performed using Cytation 5 imager (Biotek Instruments) gathering signal intensity from brightfield, YFP (for Venus fluorescence) CFP 450/440 (for Cerulean fluorescence) and Texas Red (for mCherry fluorescence) channels. Raw data processing and image analysis were performed using Gen5 3.05 software (Biotek Instruments). Briefly, the stitching of 2□×□2 montage images and Z-projection of 6 layers using focus stacking was performed on raw images followed by spheroid area analysis. For cell count calculations, a standard curve was created by measuring the area of spheroids after plating at different cell numbers 24 hours after plating. A resulting equation by fitting a curve to the data was performed by Graphpad (second order polynomial – quadratic – curve fit used). Whole spheroid area and

fluorescence intensity measurements of each population were integrated into the fitted equation, and cell counts for each population were produced as fluorescence intensities relative to spheroid size. All coculture experiments were performed in triplicates.

<u>Mathematical modeling – FACT Analysis</u>

Facilitation Analysis through Combination Therapy: The FACT algorithm breaks into six steps, which we outline here before describing in detail below. Modifiers refer to estrogen pathway modifying treatments, including estradiol itself and three ER antagonists: fulvestrant, tamoxifen, and raloxifene.

1. **Fit growth and carrying capacity** for each cell type in monoculture with no treatment.
2. **Treatment effects:** Using the carrying capacity in the absence of treatment, find the effects of ribociclib or modifier treatment on cell growth and death rates.
3. **Synergy:** From growth with combined ribociclib and modifier treatment, compare observed growth with that expected under a null model without interaction.
4. **Competition coefficients:** Using the carrying capacities and growth in sensitive and resistance cells from Step 1, estimate competition coefficients between the two cell types.
5. **Facilitation:** Using the carrying capacities, growth and death rates of single cell types with or without ribociclib from Steps 1 and 2, and the competition coefficients in the absence of treatment from Step 3, quantify facilitation as deviations of growth from predicted under a null model. To quantify facilitation in the presence of modifier we follow the same steps but with modifier treatment.
6. **Facilitation modification:** Using the growth of cells in competition with ribociclib (Step 5) and the direct effects of modifier (Step 2), quantify whether the modifier enhances or reduces facilitation.

Detailed mathematical methods

We fit each model with least squares, using all three replicates and the observed mean on day 4 for the initial condition. We exclude the measurements before day 4 because the cells show a lag before beginning their growth.

1. Fit growth and carrying capacity to single cell data in the absence of treatment. We use the logistic model, as defined by the differential equations for sensitive and resistant cells

$$\frac{dS}{dt} = r_S\left(1 - \frac{S}{K_S}\right)$$

$$\frac{dR}{dt} = r_R(1 - \frac{R}{K_R})$$

to estimate r_S, r_R, K_S and K_R as the growth rates and carrying capacities of sensitive (S) cells and resistant (R) cells.

2. Treatment and modifier effects: Using the carrying capacity in the absence of treatment we estimate growth with treatment (r_{ST} , r_{RT}) as shown, and with modifer (r_{SM} , r_{RM}) with the model

$$\frac{dS}{dt} = r_{ST}\left(1 - \frac{S}{K_S}\right)$$
$$\frac{dR}{dt} = r_{RT}\left(1 - \frac{R}{K_R}\right)$$

3. Synergy: To quantify how ribociclib interacts with modifiers in monoculture, we fit the logistic model using carrying capacities from Step 1, and compare the estimated growth r_c with the null model

$$r_S(\frac{r_{ST}}{r_S})(\frac{r_{SM}}{r_S})$$

4. Estimate competition coefficients: Using the estimates of the growth rates and carrying capacities from Step 1, we fit untreated coculture data to a Lotka-Volterra competition model with competition coefficients α_{SR} and α_{RS}

$$\frac{dS}{dt} = r_S\left(1 - \frac{S + \alpha_{SR}R}{K_S}\right)$$

$$\frac{dR}{dt} = r_R\left(1 - \frac{\alpha_{RS}S + R}{K_S}\right)$$

5. Estimate facilitation: We estimate facilitation as the deviation between observed and expected growth. To find expected growth, we use the estimates of the growth rates in monoculture with treatment, carrying capacities from the untreated monoculture, and the competition coefficients from the untreated cocultures. We fit observed growth with the baseline model.

6. Facilitation modification: If the presence of the other cell type enhances growth in the presence of ribociclib, a modifier could cancel or enhance this effect. To quantify, we use the growth parameter from step 4 in the presence of ribociclib, and account for the direct effects of the modifier as in step 2.

<u>Facilitation Analysis by Combination Therapy – Mechanistic model:</u>

Facilitation factor production, flux and utilization

To describe the mechanisms of facilitation between resistant (R) and sensitive (S) cells, we model the intracellular concentration of the facilitation factor (E) in each cell type (E_S, E_R) , and the flux of this factor between cell types via the shared extra-cellular environment (E_E). We describe the intracellular production of this factor by sensitive and resistant cells at rate ρ_S and ρ_R and the receptor binding for utilisation as a growth promoting signal at rate μ_S and μ_R. Facilitation factors diffuse between cells types and the extra-cellular environment at rate η. Finally, we describe the influx (σ_E) and decay (δ_E) of facilitation factors from the external environment. This leads to the following set of differential equations describing cellular and environmental concentrations of facilitation factors:

$$\frac{dE_S}{dt} = \rho_S + \eta(E_E - E_S) - \mu_S E_S$$

$$\frac{dE_R}{dt} = \rho_R + \eta(E_E - E_R) - \mu_R E_R$$

$$\frac{dE_E}{dt} = \sigma_E + \eta(E_S - E_E) + \eta(E_R - E_E) - \delta_E E_E.$$

The equilibrium of this system is:

$$E_E^* = \frac{\sigma_E + \rho_S S \frac{\eta}{\eta + \mu_S} + \rho_R R \frac{\eta}{\eta + \mu_R}}{\eta S \frac{\mu_S}{\eta + \mu_S} + \eta R \frac{\mu_R}{\eta + \mu_R} + \delta_E}$$

$$E_S = \frac{\rho_S + \eta E_E^*}{\eta + \mu_S}$$

$$E_R = \frac{\rho_R + \eta E_E^*}{\eta + \mu_R},$$

showing that the intra- and extracellular concentrations depend on the net balance between sources and sinks of facilitation factors. Inhibitors of the production of facilitation factors will reduce the intra and extracellular inputs to E (σ and ρ). In contrast drugs targeting facilitation factor receptors will reduce the binding of intracellular factors, reducing μ by some factor.

Coupling facilitation factor dynamics with cancer co-culture spheroid growth

The cellular level description of facilitation was next scaled to describe the populations of resistant and sensitive cells competing and facilitating in co-culture spheroids over time. The resistant and sensitive cells are described as transitioning between proliferative (P), quiescent (Z) and senescent (X) states.

Resource competition between all cells is described by the following term:

$$\alpha(P, Z, X) = 1 - \sum_{i=1}^{n} \frac{P_i + Z_i + X_i}{K_i},$$

where competitive ability of each cell type (i) is determined by the carrying capacity parameter K_i.

Proliferative cells enter the G1/S phase cell cycle checkpoint at a baseline rate (r), which is reduced by resource competition and increased by facilitation factor availability (E). This

beneficial facilitation factor effect saturates at high concentrations when uptake and binding becomes rate limited (c). The proliferation rate of resistant and sensitive cells will be related to the binding of intracellularly available facilitation factors ($\mu_i E_i$). The G1/S phase entry of cells of type i, based on competition and the internal concentration of facilitation factors therefore follows:

$$G_i = r_i(1 + \frac{\mu_i E_i}{1 + c\mu_i E_i})\alpha(P, Z, X)$$

After entering the cell cycle checkpoint, cells undertake the decision to divide or enter a quiescent state, based on the balance of key regulatory cell cycle promoters and inhibitors. In addition to a baseline quiescence rate (λ_i), cells are promoted to enter the quiescent state by the cell cycle inhibitor ribociclib (x), which inactivates the key regulators of the G1/S phase cell cycle checkpoint (CDK4/6), blocking cell cycle progression. We describe the effect of ribociclib in inhibiting cell cycle progression and driving cells into a quiescent state as increasing with drug concentration following:

$$q_i(x) = \frac{x}{k_i + x}.$$

No additional quiescence is induced in the absence of treatment, complete cell cycle arrest is achieved at very high levels of ribociclib and the half maximal cell cycle arrest is achieved at a dose $k_i$for cell type i. Differences in this parameter between resistant and sensitive cells describes innate resistance to the drug that emerged through selection. Following quiescence, we describe the transition of cells into a senescent state at rate φ_i before cell death occurs at rate δ_i.

Combining these models of competition, facilitation, cell cycle progression, arrest and cell death yields the following spheroid population model, describing the abundance of proliferative quiescent and senescent resistant and sensitive cells in co-culture spheroids over time. The dynamics of the extracellular facilitation factor concentration in the spheroid population model is governed by the balance between net secretion by proliferative and quiescent cells (resistant= γ_R and sensitive= γ_S) and its decay (δ_E), giving:

$$\frac{dP_i}{dt} = (\, G_i\big(1 - q_i(x)\big) - \, G_i q_i(x) - \, \lambda_i)P_i$$
$$\frac{dZ_i}{dt} = \, (G_i q_i(x) - \, \lambda_i)P_i - \, \varphi_i Z_i$$
$$\frac{dX_i}{dt} = \, \varphi_i Z_i - \, \delta_i X_i$$
$$\frac{dE_E}{dt} = \, \Big(\sum \gamma_i(P_i + \, Z_i)\Big) - \, \delta_E E_E.$$

Resistant and sensitive cell co-culture spheroid growth and facilitation across drug doses

Resistant and sensitive cells were fluorescently labelled and replicate populations (n=3) were plated either in monoculture or in 50:50 initial co-culture. Cancer spheroids were grown in 3D culture for 21 days, as described previously in methods (***Mono- and coculture spheroid experiments***). Imaging was performed at 3 day intervals and the abundance of each cell type enumerated as described in (PMID: **32565737)**. To explore the consequence of cell-cell interactions of drug response, the replicated mono- and co-culture time course experiments were conducted under 8 ribociclib concentrations within the EC20-50 range (0,100,200,400,600,800,1000,2000nM). Spheroid analysis and cell counts performed as described previously in methods (***Mono- and coculture spheroid experiments*****)**

Measuring the strength of competitive and facilitative interactions between subclones and vital cellular rates

We measured the strength of competitive and facilitative interactions between subclones, the drug impacts on cell cycle arrest and the vital cellular rates of proliferation, quiescence and senescence, by fitting the spheroid population model to the experimental data described above. Given the initial spheroid size and composition and the ribociclib concentration, the spheroid population model projects the abundance of sensitive and resistant cells throughout the experiment based on a given combination of biological rates. A log normal distribution measurement model was used to evaluate the likelihood of each spheroid abundance observation and weakly informative priors were used in all cases (Supplemental methods). The biological rates of each process in the spheroid population model were inferred with uncertainty, using Bayesian Hamiltonian Monte Carlo (HMC) (70). Biological rates were identified that yield the most accurate model predictions of the observed spheroid growth trajectories and composition over time and across all drug doses. The HMC algorithm efficiently samples the posterior distribution, desrcibing the likely biological rates given the model, using derivatives of the probability density function. As a result, the inference approach jointly and efficiently: i) identifies the most probable range of subclone interaction strengths (competition and facilitation), ii) predicts the cellular composition and facilitation factor concentration throughout the experiments and iii) provides a probabilistic measurement of the likelihood of the hypothesis encoded by the model given the available data.

Comparing alternative hypotheses (models) of the mechanisms generating spheroid growth

We assessed the support for the hypothesis that facilitation is playing an important role in influencing the growth of spheroids containing resistant and sensitive cells. We generated a range of alternative hypotheses about processes that could generate the spheroid growth dynamics and formally compared the performance of these models at explaining the data, after each was fitted to the data (as described above). Specifically, we developed alternative population level models hypothesizing that the spheroid growth trajectories and composition were driven by:

a) Competition alone: Resistant and sensitive cells have differing proliferation and death rates and compete.

b) Plasticity (D): Drug induced phenotypic plasticity inducing a transition of both cell types to a more resistant state. Cells in all states compete and differ in birth and death rates.
c) Plasticity (RS): Random phenotypic switching of both cell types between a more and less susceptible state. Cells in all states compete and differ in birth and death rates.
d) Facilitation Symmetric (1D): Facilitation of equal strength between resistant and sensitive (Allee effect model). Cells in all states compete and differ in birth and death rates
e) Facilitation (1D): Facilitation where resistant and sensitive cells contribute differently to the production of a growth promoting signal. Cells in all states compete and differ in birth and death rates
f) Facilitation (2D): Facilitation where resistant and sensitive cells contribute differently to the production of a growth promoting signal and ribociclib treatment induces senescence. Cells in all states compete and differ in birth and death rates
g) Facilitation (3D) (the full model): Facilitation where resistant and sensitive cells contribute differently to the production of a growth promoting signal and ribociclib treatment induces quiescence and then senescence. Cells in all states compete and differ in birth and death rates

The support for each hypothesis was measured by calculating the penalized prediction error of each model, using WAIC (widely applicable information criterion) to avoiding overfitting the data by penalizing the model likelihood based on model complexity.

Model predictions of final spheroid size when modulating the strength of facilitation

To explore the consequences of blocking facilitation, we analyzed the impact on resistant and sensitive cell abundances of reducing the rate of receptor binding with facilitation factors. The most likely values of the receptor binding parameters of each cell type (μ_S and μ_R) were reduced by a factor ζ (between 0 and 80% reduction). Using the model and holding all other parameters constant, the predicted abundance of sensitive and resistant cells after 21 days of co-culture was forecasted, assuming continuous facilitation blocking throughout this period.

<u>Liquid chromatography-tandem mass spectrometry (LC-MS/MS)</u>

Media samples taken at day 21 from 3D spheroid experiments, treated with or without ribociclib, (experimental setup previously described in results and methods - ***Mono- and coculture 3D spheroid experiments***) and plated in different compositions (100% sensitive, 50% sensitive – 50% resistant, and 100% resistant) were spun down at 300g and frozen at -80 ^{o}C. Samples were then prepared by the Analytical Cytometry Core of City of Hope National Medical Center for LC-MS/MS for estrone and estradiol detection. LC-MS/MS system consisted of a Shimadzu Prominence HPLC system interfaced to an AB SCIEX QTRAP® 5500 system (Foster City, CA, USA). HPLC separation was achieved using a XSELECT CSH Phenyl-Hexyl 3.5um, 2.1x150mm analytical column (Waters) The column temperature was maintained at 50°C, and the flow rate was 0.38ml/min. The mobile phase consisted of A (Water: 1000ml + 60ul 30%NH4OH) and B (Methanol : 1000ml+ 60ul 30% NH4OH). The following gradient program was used: 55% B (0.01 min), 70% B (0.01-4.0 min), 100% B (5.5min), 30%B (8.5min) The total run time was 8.5min. The auto-injector temperature was maintained at 15 ^{o}C. The atmospheric pressure chemical ionization (APCI)source of the mass spectrometer was operated in negative

ion mode with ion source gas1 (55), curtain gas (20), collision gas (High), nebulizer current -4.0, The entrance potential was set to -10V. Declustering potential (DP) was -110, collision energy (CE), and collision cell exit potential (CXP) was optimized to -50V, -21V for Estrone, -160V, -50V,-17V for Estrone internal standard), -210V,-58V,-19V for Estradiol and --205V,-52V, -13V for Estradiol internal standard respectively. The source temperature was 400 ^{o}C. A solvent delay program was used from 0 to 3.5 min and from 6.5 to 8.5min to minimize the mobile phase flow to the source. Analyst software version 1.5.1 was used for data acquisition and processing. Atmospheric – pressure chemical. ionization of Estrone, Estrone D4 , Estradiol , Estradiol D5 produced abundant protonated molecular ions (MH-) at m/z 268.980, 272.983, 270.969,and 275.981 respectively. Fragmentation of these compounds was induced under collision induced dissociation conditions. The precursor→product ion combinations at m/z 268.980→145.200 for Estrone, and 272.983→147.100 for Estrone-I.S. 270.969→182.800 and 275.981→147.000 for Estradiol and Estradiol-IS were used in multiple-reaction monitoring mode for quantitation. Under optimized assay conditions, the retention times for Estrone, Estrone IS and Estradiol, Estradiol -IS. were 4.89, 4.60 min, respectively.

<u>Multiplex cytokine analysis</u>

Media samples taken at day 21 from 3D spheroid experiments, treated with or without ribociclib, (experimental setup previously described in results and methods - ***Mono- and coculture 3D spheroid experiments***) and plated in different compositions (100% sensitive, 50% sensitive – 50% resistant, and 100% resistant) were spun down at 300g and frozen at -80 ^{o}C. Samples were then prepared by the Analytical Cytometry Core of City of Hope National Medical Center for multiplex cytokine analysis. Samples were analyzed for 5 cytokines (EGF, FGF-2, FGF-21, FGF-23, and TGFα) using the "ProcartaPlex Multiplex Immunoassay Kit" (Invitrogen, Camarillo, CA) per manufacturer's protocol. In addition, TGFβ-1, -2, and -3 were measured using the "Magnetic Luminex Performance Assay Kit" (R&D Systems, Minneapolis MN) also according to manufacturer's instructions. For analysis of TGFβ, the latent proteins required activation to their immunoreactive state prior to detection. Activation was accomplished by adding 20 µl of 1N HCl to 100 µl of sample followed by incubation for 10 minutes at room temperature. Samples were then neutralized by the addition of 20 µl of 1.2N NaOH/0.5M HEPES prior to dilution and loading on to the plate. Briefly, multiplex bead solutions were vortexed for 30 s and 50 µl was added to each well and then washed twice with wash buffer. Next, 50 µl of sample (cell culture supernatant) was loaded in duplicate into Greiner flat-bottom 96 well microplates. Cytokines standards were reconstituted with unconditioned cell culture medium and serial dilutions were prepared. Plates were then incubated on a plate shaker at 500 rpm in the dark at room temperature for 2 hours. The plate was then applied to a magnetic device designed to accommodate a microplate and all wells were washed two times with 200 µl of wash buffer. Biotinylated detection antibody mix (25 µl) was added to each well and the plate was incubated on the plate shaker for another hour. After washing two times with 200 µl of wash buffer, streptavidin-phycoerythrin (50 µl) was added to each well followed by incubation on a plate shaker for 30 minutes. After two more washes, the contents of each well were resuspended in 120 µl reading buffer and shaken for 5 min. Finally, the plate was transferred to the Flexmap

3D Luminex system (Luminex corp.) for analysis, Cytokine concentrations were calculated using Bio-Plex Manager 6.2 software with a five parameter curve-fitting algorithm applied for standard curve calculations for duplicate samples.

References:

1. McGranahan N, Swanton C. Clonal Heterogeneity and Tumor Evolution: Past, Present, and the Future. Cell. 2017;168(4):613-28. doi: 10.1016/j.cell.2017.01.018. PubMed PMID: 28187284.
2. Delou JMA, Souza ASO, Souza LCM, Borges HL. Highlights in Resistance Mechanism Pathways for Combination Therapy. Cells. 2019;8(9). doi: 10.3390/cells8091013. PubMed PMID: 31480389; PMCID: 6770082.
3. Fedele C, Tothill RW, McArthur GA. Navigating the challenge of tumor heterogeneity in cancer therapy. Cancer discovery. 2014;4(2):146-8. doi: 10.1158/2159-8290.CD-13-1042. PubMed PMID: 24501303.
4. Swanton C. Intratumor heterogeneity: evolution through space and time. Cancer research. 2012;72(19):4875-82. doi: 10.1158/0008-5472.CAN-12-2217. PubMed PMID: 23002210; PMCID: 3712191.
5. Brady SW, McQuerry JA, Qiao Y, Piccolo SR, Shrestha G, Jenkins DF, Layer RM, Pedersen BS, Miller RH, Esch A, Selitsky SR, Parker JS, Anderson LA, Dalley BK, Factor RE, Reddy CB, Boltax JP, Li DY, Moos PJ, Gray JW, Heiser LM, Buys SS, Cohen AL, Johnson WE, Quinlan AR, Marth G, Werner TL, Bild AH. Combating subclonal evolution of resistant cancer phenotypes. Nat Commun. 2017;8(1):1231. Epub 2017/11/03. doi: 10.1038/s41467-017-01174-3. PubMed PMID: 29093439; PMCID: PMC5666005.
6. Beckman RA, Loeb LA. Evolutionary dynamics and significance of multiple subclonal mutations in cancer. DNA repair. 2017;56:7-15. doi: 10.1016/j.dnarep.2017.06.002. PubMed PMID: 28652129; PMCID: 5551892.
7. Kim C, Gao R, Sei E, Brandt R, Hartman J, Hatschek T, Crosetto N, Foukakis T, Navin NE. Chemoresistance Evolution in Triple-Negative Breast Cancer Delineated by Single-Cell Sequencing. Cell. 2018;173(4):879-93 e13. doi: 10.1016/j.cell.2018.03.041. PubMed PMID: 29681456; PMCID: 6132060.
8. Gluckman PD, Low FM, Buklijas T, Hanson MA, Beedle AS. How evolutionary principles improve the understanding of human health and disease. Evolutionary applications. 2011;4(2):249-63. doi: 10.1111/j.1752-4571.2010.00164.x. PubMed PMID: WOS:000287451800007.
9. Gatenby RA, Vincent TL. Application of quantitative models from population biology and evolutionary game theory to tumor therapeutic strategies. Molecular cancer therapeutics. 2003;2(9):919-27. PubMed PMID: 14555711.
10. Sieber OM, Tomlinson SR, Tomlinson IP. Tissue, cell and stage specificity of (epi)mutations in cancers. Nature reviews Cancer. 2005;5(8):649-55. doi: 10.1038/nrc1674. PubMed PMID: 16056260.
11. Crespi B, Summers K. Evolutionary biology of cancer. Trends in ecology & evolution. 2005;20(10):545-52. doi: 10.1016/j.tree.2005.07.007. PubMed PMID: 16701433.

12. Pienta KJ, McGregor N, Axelrod R, Axelrod DE. Ecological therapy for cancer: defining tumors using an ecosystem paradigm suggests new opportunities for novel cancer treatments. Translational oncology. 2008;1(4):158-64. doi: 10.1593/tlo.08178. PubMed PMID: 19043526; PMCID: 2582164.
13. Heppner GH. Cancer cell societies and tumor progression. Stem cells. 1993;11(3):199-203. doi: 10.1002/stem.5530110306. PubMed PMID: 8318906.
14. Gatenby RA, Brown JS. The Evolution and Ecology of Resistance in Cancer Therapy. Cold Spring Harbor perspectives in medicine. 2020;10(11). doi: 10.1101/cshperspect.a040972. PubMed PMID: 33139405; PMCID: 7605238.
15. Franco OE, Tyson DR, Konvinse KC, Udyavar AR, Estrada L, Quaranta V, Crawford SE, Hayward SW. Altered TGF-alpha/beta signaling drives cooperation between breast cancer cell populations. FASEB journal : official publication of the Federation of American Societies for Experimental Biology. 2016;30(10):3441-52. doi: 10.1096/fj.201500187RR. PubMed PMID: 27383183; PMCID: 5024699.
16. Adler FR, Gordon DM. Cancer Ecology and Evolution: Positive interactions and system vulnerability. Current opinion in systems biology. 2019;17:1-7. doi: 10.1016/j.coisb.2019.09.001. PubMed PMID: 32318644; PMCID: 7172748.
17. Bhang HE, Ruddy DA, Krishnamurthy Radhakrishna V, Caushi JX, Zhao R, Hims MM, Singh AP, Kao I, Rakiec D, Shaw P, Balak M, Raza A, Ackley E, Keen N, Schlabach MR, Palmer M, Leary RJ, Chiang DY, Sellers WR, Michor F, Cooke VG, Korn JM, Stegmeier F. Studying clonal dynamics in response to cancer therapy using high-complexity barcoding. Nature medicine. 2015;21(5):440-8. doi: 10.1038/nm.3841. PubMed PMID: 25849130.
18. Martin-Pardillos A, Valls Chiva A, Bande Vargas G, Hurtado Blanco P, Pineiro Cid R, Guijarro PJ, Hummer S, Bejar Serrano E, Rodriguez-Casanova A, Diaz-Lagares A, Castellvi J, Miravet-Verde S, Serrano L, Lluch-Senar M, Sebastian V, Bribian A, Lopez-Mascaraque L, Lopez-Lopez R, Ramon YCS. The role of clonal communication and heterogeneity in breast cancer. BMC cancer. 2019;19(1):666. doi: 10.1186/s12885-019-5883-y. PubMed PMID: 31277602; PMCID: 6612119.
19. Bowling S, Lawlor K, Rodriguez TA. Cell competition: the winners and losers of fitness selection. Development. 2019;146(13). doi: 10.1242/dev.167486. PubMed PMID: 31278123.
20. Madan E, Peixoto ML, Dimitrion P, Eubank TD, Yekelchyk M, Talukdar S, Fisher PB, Mi QS, Moreno E, Gogna R. Cell Competition Boosts Clonal Evolution and Hypoxic Selection in Cancer. Trends in cell biology. 2020;30(12):967-78. doi: 10.1016/j.tcb.2020.10.002. PubMed PMID: 33160818.
21. Zhou H, Neelakantan D, Ford HL. Clonal cooperativity in heterogenous cancers. Seminars in cell & developmental biology. 2017;64:79-89. doi: 10.1016/j.semcdb.2016.08.028. PubMed PMID: 27582427; PMCID: 5330947.
22. Kanarek AR, Webb CT. Allee effects, adaptive evolution, and invasion success. Evolutionary applications. 2010;3(2):122-35. doi: 10.1111/j.1752-4571.2009.00112.x. PubMed PMID: 25567913; PMCID: 3352477.
23. Vazquez DP, Ramos-Jiliberto R, Urbani P, Valdovinos FS. A conceptual framework for studying the strength of plant-animal mutualistic interactions. Ecology letters. 2015;18(4):385-400. doi: 10.1111/ele.12411. PubMed PMID: 25735791.
24. Kefi S, van Baalen M, Rietkerk M, Loreau M. Evolution of local facilitation in arid ecosystems. The American naturalist. 2008;172(1):E1-17. doi: 10.1086/588066. PubMed PMID: 18554137.
25. Bertness MD, Callaway R. Positive interactions in communities. Trends in ecology & evolution. 1994;9(5):191-3. doi: 10.1016/0169-5347(94)90088-4. PubMed PMID: 21236818.
26. Axelrod R, Axelrod DE, Pienta KJ. Evolution of cooperation among tumor cells. Proceedings of the National Academy of Sciences of the United States of America. 2006;103(36):13474-9. doi: 10.1073/pnas.0606053103. PubMed PMID: 16938860; PMCID: 1557388.

27. Cleary AS, Leonard TL, Gestl SA, Gunther EJ. Tumour cell heterogeneity maintained by cooperating subclones in Wnt-driven mammary cancers. Nature. 2014;508(7494):113-7. doi: 10.1038/nature13187. PubMed PMID: 24695311; PMCID: 4050741.
28. Maley CC, Aktipis A, Graham TA, Sottoriva A, Boddy AM, Janiszewska M, Silva AS, Gerlinger M, Yuan Y, Pienta KJ, Anderson KS, Gatenby R, Swanton C, Posada D, Wu CI, Schiffman JD, Hwang ES, Polyak K, Anderson ARA, Brown JS, Greaves M, Shibata D. Classifying the evolutionary and ecological features of neoplasms. Nature reviews Cancer. 2017;17(10):605-19. doi: 10.1038/nrc.2017.69. PubMed PMID: 28912577; PMCID: 5811185.
29. Archetti M. Cooperation between cancer cells. Evolution, medicine, and public health. 2018;2018(1):1. doi: 10.1093/emph/eoy003. PubMed PMID: 29410785; PMCID: 5793724.
30. Oates K, Wilson M. Nominal kinship cues facilitate altruism. Proceedings Biological sciences. 2002;269(1487):105-9. doi: 10.1098/rspb.2001.1875. PubMed PMID: 11798424; PMCID: 1690876.
31. Wilson DS, Pollock GB, Dugatkin LA. Can Altruism Evolve in Purely Viscous Populations. Evol Ecol. 1992;6(4):331-41. doi: Doi 10.1007/Bf02270969. PubMed PMID: WOS:A1992JD08100005.
32. Bruno JF, Stachowicz JJ, Bertness MD. Inclusion of facilitation into ecological theory. Trends in ecology & evolution. 2003;18(3):119-25. doi: Pii S0169-5347(02)00045-9
Doi 10.1016/S0169-5347(02)00045-9. PubMed PMID: WOS:000181729900007.
33. Caldwell MM, Dawson TE, Richards JH. Hydraulic lift: Consequences of water efflux from the roots of plants. Oecologia. 1998;113(2):151-61. doi: DOI 10.1007/s004420050363. PubMed PMID: WOS:000071658500001.
34. de Mazancourt C, Schwartz MW. A resource ratio theory of cooperation. Ecology letters. 2010;13(3):349-59. doi: 10.1111/j.1461-0248.2009.01431.x. PubMed PMID: 20455920.
35. Leigh EG, Jr. The evolution of mutualism. Journal of evolutionary biology. 2010;23(12):2507-28. doi: 10.1111/j.1420-9101.2010.02114.x. PubMed PMID: 20942825.
36. Tabassum DP, Polyak K. Tumorigenesis: it takes a village. Nature reviews Cancer. 2015;15(8):473-83. doi: 10.1038/nrc3971. PubMed PMID: 26156638.
37. Travis JM, Brooker RW, Dytham C. The interplay of positive and negative species interactions across an environmental gradient: insights from an individual-based simulation model. Biology letters. 2005;1(1):5-8. doi: 10.1098/rsbl.2004.0236. PubMed PMID: 17148114; PMCID: 1629044.
38. Deisboeck TS, Couzin ID. Collective behavior in cancer cell populations. Bioessays. 2009;31(2):190-7. doi: 10.1002/bies.200800084. PubMed PMID: WOS:000263863600009.
39. Azuma K, Kawahara A, Sonoda K, Nakashima K, Tashiro K, Watari K, Izumi H, Kage M, Kuwano M, Ono M, Hoshino T. FGFR1 activation is an escape mechanism in human lung cancer cells resistant to afatinib, a pan-EGFR family kinase inhibitor. Oncotarget. 2014;5(15):5908-19. doi: 10.18632/oncotarget.1866. PubMed PMID: 25115383; PMCID: 4171601.
40. Janiszewska M, Tabassum DP, Castano Z, Cristea S, Yamamoto KN, Kingston NL, Murphy KC, Shu S, Harper NW, Del Alcazar CG, Aleckovic M, Ekram MB, Cohen O, Kwak M, Qin Y, Laszewski T, Luoma A, Marusyk A, Wucherpfennig KW, Wagle N, Fan R, Michor F, McAllister SS, Polyak K. Subclonal cooperation drives metastasis by modulating local and systemic immune microenvironments. Nature cell biology. 2019;21(7):879-88. doi: 10.1038/s41556-019-0346-x. PubMed PMID: 31263265; PMCID: 6609451.
41. Rozeboom B, Dey N, De P. ER+ metastatic breast cancer: past, present, and a prescription for an apoptosis-targeted future. American journal of cancer research. 2019;9(12):2821-31. PubMed PMID: 31911865; PMCID: 6943351.
42. Harvey JM, Clark GM, Osborne CK, Allred DC. Estrogen receptor status by immunohistochemistry is superior to the ligand-binding assay for predicting response to adjuvant endocrine therapy in breast cancer. J Clin Oncol. 1999;17(5):1474-81. doi: Doi 10.1200/Jco.1999.17.5.1474. PubMed PMID: WOS:000080267900020.

43. Rani A, Stebbing J, Giamas G, Murphy J. Endocrine Resistance in Hormone Receptor Positive Breast Cancer-From Mechanism to Therapy. Front Endocrinol (Lausanne). 2019;10:245. Epub 2019/06/11. doi: 10.3389/fendo.2019.00245. PubMed PMID: 31178825; PMCID: PMC6543000.
44. Zhao H, Zhou L, Shangguan AJ, Bulun SE. Aromatase expression and regulation in breast and endometrial cancer. J Mol Endocrinol. 2016;57(1):R19-33. Epub 2016/04/14. doi: 10.1530/jme-15-0310. PubMed PMID: 27067638; PMCID: PMC5519084.
45. Osborne CK. Tamoxifen in the treatment of breast cancer. N Engl J Med. 1998;339(22):1609-18. Epub 1998/11/26. doi: 10.1056/nejm199811263392207. PubMed PMID: 9828250.
46. Effects of chemotherapy and hormonal therapy for early breast cancer on recurrence and 15-year survival: an overview of the randomised trials. Lancet. 2005;365(9472):1687-717. Epub 2005/05/17. doi: 10.1016/s0140-6736(05)66544-0. PubMed PMID: 15894097.
47. Company ELa. Endocrine Therapy With or Without Abemaciclib (LY2835219) Following Surgery in Participants With Breast Cancer (monarchE) 2017 [updated September 18, 2020; cited 2020 October 13]. Available from: https://www.clinicaltrials.gov/ct2/show/NCT03155997.
48. Pharmaceuticals N. A Trial to Evaluate Efficacy and Safety of Ribociclib With Endocrine Therapy as Adjuvant Treatment in Patients With HR+/HER2- Early Breast Cancer (NATALEE) 2018 [updated October 2, 2020; cited 2020 October 13]. Available from: https://clinicaltrials.gov/ct2/show/NCT03701334.
49. Bertagnolli M ME, DeMichele A, Gnant M. PALbociclib CoLlaborative Adjuvant Study (PALLAS) 2015 [updated March 9, 2020; cited 2020 October 2013]. Available from: https://clinicaltrials.gov/ct2/show/NCT02513394.
50. PENELOPE-B TRIAL OF IBRANCE® (PALBOCICLIB) IN EARLY BREAST CANCER DID NOT MEET PRIMARY ENDPOINT: Pfizer; 2020 [updated October 9, 2020; cited 2020 October 13]. Available from: https://www.pfizer.com/news/press-release/press-release-detail/penelope-b-trial-ibrancer-palbociclib-early-breast-cancer.
51. Johnston S, Puhalla S, Wheatley D, Ring A, Barry P, Holcombe C, Boileau JF, Provencher L, Robidoux A, Rimawi M, McIntosh SA, Shalaby I, Stein RC, Thirlwell M, Dolling D, Morden J, Snowdon C, Perry S, Cornman C, Batten LM, Jeffs LK, Dodson A, Martins V, Modi A, Osborne CK, Pogue-Geile KL, Cheang MCU, Wolmark N, Julian TB, Fisher K, MacKenzie M, Wilcox M, Huang Bartlett C, Koehler M, Dowsett M, Bliss JM, Jacobs SA. Randomized Phase II Study Evaluating Palbociclib in Addition to Letrozole as Neoadjuvant Therapy in Estrogen Receptor-Positive Early Breast Cancer: PALLET Trial. J Clin Oncol. 2019;37(3):178-89. Epub 2018/12/14. doi: 10.1200/jco.18.01624. PubMed PMID: 30523750.
52. Johnston SRD, Harbeck N, Hegg R, Toi M, Martin M, Shao ZM, Zhang QY, Martinez Rodriguez JL, Campone M, Hamilton E, Sohn J, Guarneri V, Okada M, Boyle F, Neven P, Cortés J, Huober J, Wardley A, Tolaney SM, Cicin I, Smith IC, Frenzel M, Headley D, Wei R, San Antonio B, Hulstijn M, Cox J, O'Shaughnessy J, Rastogi P. Abemaciclib Combined With Endocrine Therapy for the Adjuvant Treatment of HR+, HER2-, Node-Positive, High-Risk, Early Breast Cancer (monarchE). J Clin Oncol. 2020;38(34):3987-98. Epub 2020/09/22. doi: 10.1200/jco.20.02514. PubMed PMID: 32954927; PMCID: PMC7768339.
53. Griffiths JI, Chen J, Winblad O, O'Dea A, Sharma P, Trivedi M, Kalinsky K, Wisinski KB, O'Regan R, Makhoul I, Yuan Y, Spring LM, Bardia A, Jahanzeb M, Adler FR, Cohen AL, Bild AH, Khan QJ. Reconstructing tumor trajectories during therapy through integration of multiple measurement modalities. bioRxiv. 2021:2021.01.14.426737. doi: 10.1101/2021.01.14.426737.
54. Grolmusz VK, Chen J, Emond R, Cosgrove PA, Pflieger L, Nath A, Moos PJ, Bild AH. Exploiting collateral sensitivity controls growth of mixed culture of sensitive and resistant cells and decreases selection for resistant cells in a cell line model. Cancer cell international. 2020;20:253. doi: 10.1186/s12935-020-01337-1. PubMed PMID: 32565737; PMCID: 7301982.

55. Jeselsohn R, De Angelis C, Brown M, Schiff R. The Evolving Role of the Estrogen Receptor Mutations in Endocrine Therapy-Resistant Breast Cancer. Curr Oncol Rep. 2017;19(5):35. Epub 2017/04/05. doi: 10.1007/s11912-017-0591-8. PubMed PMID: 28374222.
56. Roberto M, Astone A, Botticelli A, Carbognin L, Cassano A, D'Auria G, Fabbri A, Fabi A, Gamucci T, Krasniqi E, Minelli M, Orlandi A, Pantano F, Paris I, Pizzuti L, Portarena I, Salesi N, Scagnoli S, Scavina P, Tonini G, Vici P, Marchetti P. CDK4/6 Inhibitor Treatments in Patients with Hormone Receptor Positive, Her2 Negative Advanced Breast Cancer: Potential Molecular Mechanisms, Clinical Implications and Future Perspectives. Cancers (Basel). 2021;13(2). Epub 2021/01/23. doi: 10.3390/cancers13020332. PubMed PMID: 33477469; PMCID: PMC7830463.
57. Cristofanilli M, Turner NC, Bondarenko I, Ro J, Im SA, Masuda N, Colleoni M, DeMichele A, Loi S, Verma S, Iwata H, Harbeck N, Zhang K, Theall KP, Jiang Y, Bartlett CH, Koehler M, Slamon D. Fulvestrant plus palbociclib versus fulvestrant plus placebo for treatment of hormone-receptor-positive, HER2-negative metastatic breast cancer that progressed on previous endocrine therapy (PALOMA-3): final analysis of the multicentre, double-blind, phase 3 randomised controlled trial. Lancet Oncol. 2016;17(4):425-39. Epub 2016/03/08. doi: 10.1016/s1470-2045(15)00613-0. PubMed PMID: 26947331.
58. Kalas W, Yu JL, Milsom C, Rosenfeld J, Benezra R, Bornstein P, Rak J. Oncogenes and Angiogenesis: down-regulation of thrombospondin-1 in normal fibroblasts exposed to factors from cancer cells harboring mutant ras. Cancer Res. 2005;65(19):8878-86. Epub 2005/10/06. doi: 10.1158/0008-5472.Can-05-1479. PubMed PMID: 16204059.
59. Hanahan D, Folkman J. Patterns and Emerging Mechanisms of the Angiogenic Switch during Tumorigenesis. Cell. 1996;86(3):353-64. doi: https://doi.org/10.1016/S0092-8674(00)80108-7.
60. Archetti M, Pienta KJ. Cooperation among cancer cells: applying game theory to cancer. Nat Rev Cancer. 2019;19(2):110-7. Epub 2018/11/25. doi: 10.1038/s41568-018-0083-7. PubMed PMID: 30470829.
61. Naffar-Abu Amara S, Kuiken HJ, Selfors LM, Butler T, Leung ML, Leung CT, Kuhn EP, Kolarova T, Hage C, Ganesh K, Panayiotou R, Foster R, Rueda BR, Aktipis A, Spellman P, Ince TA, Xiu J, Oberley M, Gatalica Z, Navin N, Mills GB, Bronson RT, Brugge JS. Transient commensal clonal interactions can drive tumor metastasis. Nat Commun. 2020;11(1):5799. Epub 2020/11/18. doi: 10.1038/s41467-020-19584-1. PubMed PMID: 33199705; PMCID: PMC7669858.
62. Archetti M, Ferraro DA, Christofori G. Heterogeneity for IGF-II production maintained by public goods dynamics in neuroendocrine pancreatic cancer. Proc Natl Acad Sci U S A. 2015;112(6):1833-8. Epub 2015/01/28. doi: 10.1073/pnas.1414653112. PubMed PMID: 25624490; PMCID: PMC4330744.
63. Simigdala N, Gao Q, Pancholi S, Roberg-Larsen H, Zvelebil M, Ribas R, Folkerd E, Thompson A, Bhamra A, Dowsett M, Martin L-A. Cholesterol biosynthesis pathway as a novel mechanism of resistance to estrogen deprivation in estrogen receptor-positive breast cancer. Breast Cancer Research. 2016;18(1):58. doi: 10.1186/s13058-016-0713-5.
64. Harada N. Aberrant expression of aromatase in breast cancer tissues. J Steroid Biochem Mol Biol. 1997;61(3-6):175-84. Epub 1997/04/01. PubMed PMID: 9365188.
65. Forbes NS, Meadows AL, Clark DS, Blanch HW. Estradiol stimulates the biosynthetic pathways of breast cancer cells: detection by metabolic flux analysis. Metab Eng. 2006;8(6):639-52. Epub 2006/08/15. doi: 10.1016/j.ymben.2006.06.005. PubMed PMID: 16904360.
66. Platet N, Cathiard AM, Gleizes M, Garcia M. Estrogens and their receptors in breast cancer progression: a dual role in cancer proliferation and invasion. Crit Rev Oncol Hematol. 2004;51(1):55-67. Epub 2004/06/23. doi: 10.1016/j.critrevonc.2004.02.001. PubMed PMID: 15207254.
67. AlFakeeh A, Brezden-Masley C. Overcoming endocrine resistance in hormone receptor-positive breast cancer. Curr Oncol. 2018;25(Suppl 1):S18-s27. Epub 2018/06/19. doi: 10.3747/co.25.3752. PubMed PMID: 29910644; PMCID: PMC6001756.

68. Gonzalez-Angulo AM, Morales-Vasquez F, Hortobagyi GN. Overview of resistance to systemic therapy in patients with breast cancer. Adv Exp Med Biol. 2007;608:1-22. Epub 2007/11/13. doi: 10.1007/978-0-387-74039-3_1. PubMed PMID: 17993229.
69. Weber K, Bartsch U, Stocking C, Fehse B. A multicolor panel of novel lentiviral "gene ontology" (LeGO) vectors for functional gene analysis. Molecular therapy : the journal of the American Society of Gene Therapy. 2008;16(4):698-706. doi: 10.1038/mt.2008.6. PubMed PMID: 18362927.
70. Carpenter B, Gelman A, Hoffman MD, Lee D, Goodrich B, Betancourt M, Brubaker MA, Guo J, Li P, Riddell A. Stan: a probabilistic programming language. Grantee Submission. 2017;76(1):1-32.

Acknowledgements

The authors would like to acknowledge the professional support of the Analytical Cytometry Core of City of Hope National Medical Center, led by Dr. Tim Synold. This research and JIG, RSS, FRA, and AHB have been supported by an NIH NCI U54CA209978 grant from the National Cancer Institute.

Author contributions

RE carried out experiments, was involved in their analysis and wrote the manuscript. JIG and FRA carried out the mathematical modeling and facilitation analysis and wrote the manuscript. VKG generated cell lines, performed experiments, and developed system for growth measurements. AHB conceived the study, was involved in data analysis, and wrote the manuscript. RS developed the preliminary mathematical models. All authors approved the final version of the manuscript.

Competing interests

The authors declare no competing interests.

Data availability

All data on which results are based and conclusions are made are presented in the paper.

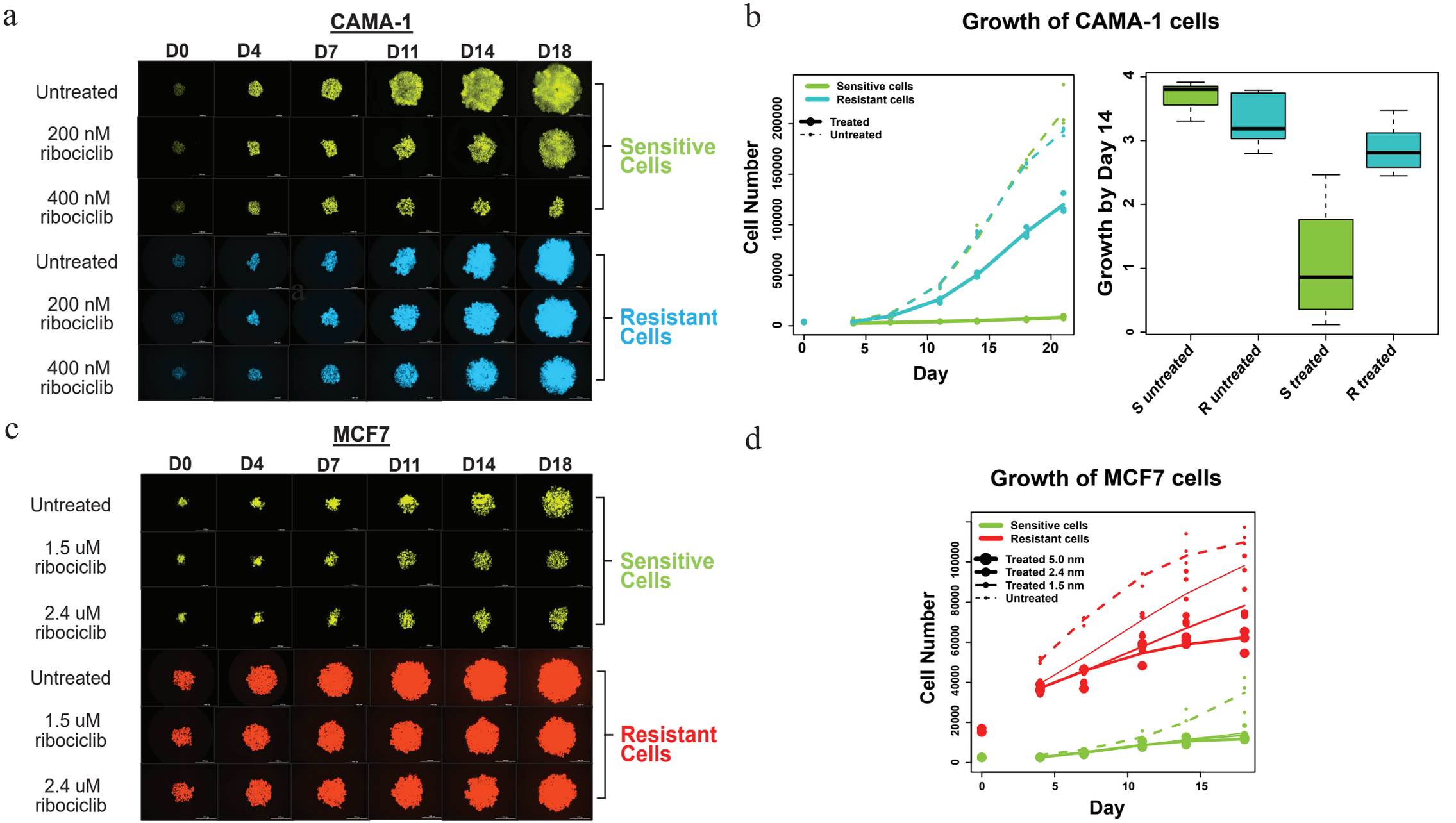

***Figure 1*. Sensitive and resistant cell growth and treatment effects. a,** CAMA-1 spheroids of 100% monoculture sensitive (venus, green) or resistant cells (cerulean, blue) cultured in untreated control, 200 nM ribociclib, and 400nM ribociclib treated medium for 18 days. Images taken at Day 18. **b,** Growth curves of CAMA-1 untreated and ribociclib treated sensitive and resistant cell populations; Box plot of CAMA-1 growth of untreated and ribociclib treated sensitive or resistant cells from day 0 to day 14 ($p < 0.0001$ for interaction between cell type and treatment with a linear model) **c,** MCF7 spheroids of 100% monoculture sensitive (venus, green) or resistant cells (mcherry, red) cultured in untreated, 1.5 uM ribociclib, and 2.4 uM ribociclib treated medium for 18 days. Images taken at Day 18. **d,** Growth curves of MCF7 untreated and ribociclib treated sensitive and resistant cell populations ($p < 0.05$ for greater reduction in growth in sensitive cells at each level of treatment based on the interaction term from a linear model of log growth between day 4 and day 18).

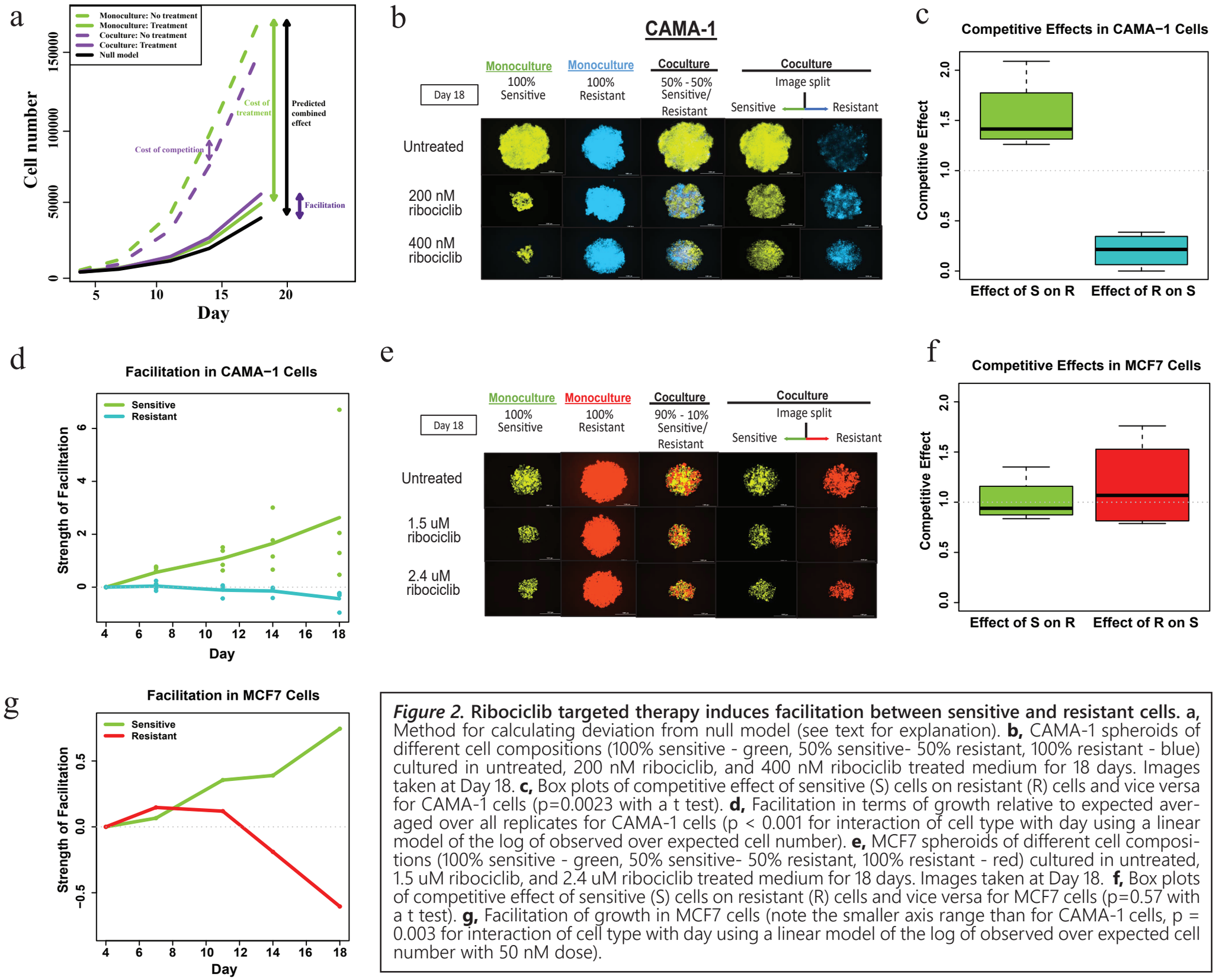

Figure 2. **Ribociclib targeted therapy induces facilitation between sensitive and resistant cells. a,** Method for calculating deviation from null model (see text for explanation). **b,** CAMA-1 spheroids of different cell compositions (100% sensitive - green, 50% sensitive- 50% resistant, 100% resistant - blue) cultured in untreated, 200 nM ribociclib, and 400 nM ribociclib treated medium for 18 days. Images taken at Day 18. **c,** Box plots of competitive effect of sensitive (S) cells on resistant (R) cells and vice versa for CAMA-1 cells ($p=0.0023$ with a t test). **d,** Facilitation in terms of growth relative to expected averaged over all replicates for CAMA-1 cells ($p < 0.001$ for interaction of cell type with day using a linear model of the log of observed over expected cell number). **e,** MCF7 spheroids of different cell compositions (100% sensitive - green, 50% sensitive- 50% resistant, 100% resistant - red) cultured in untreated, 1.5 uM ribociclib, and 2.4 uM ribociclib treated medium for 18 days. Images taken at Day 18. **f,** Box plots of competitive effect of sensitive (S) cells on resistant (R) cells and vice versa for MCF7 cells ($p=0.57$ with a t test). **g,** Facilitation of growth in MCF7 cells (note the smaller axis range than for CAMA-1 cells, $p = 0.003$ for interaction of cell type with day using a linear model of the log of observed over expected cell number with 50 nM dose).

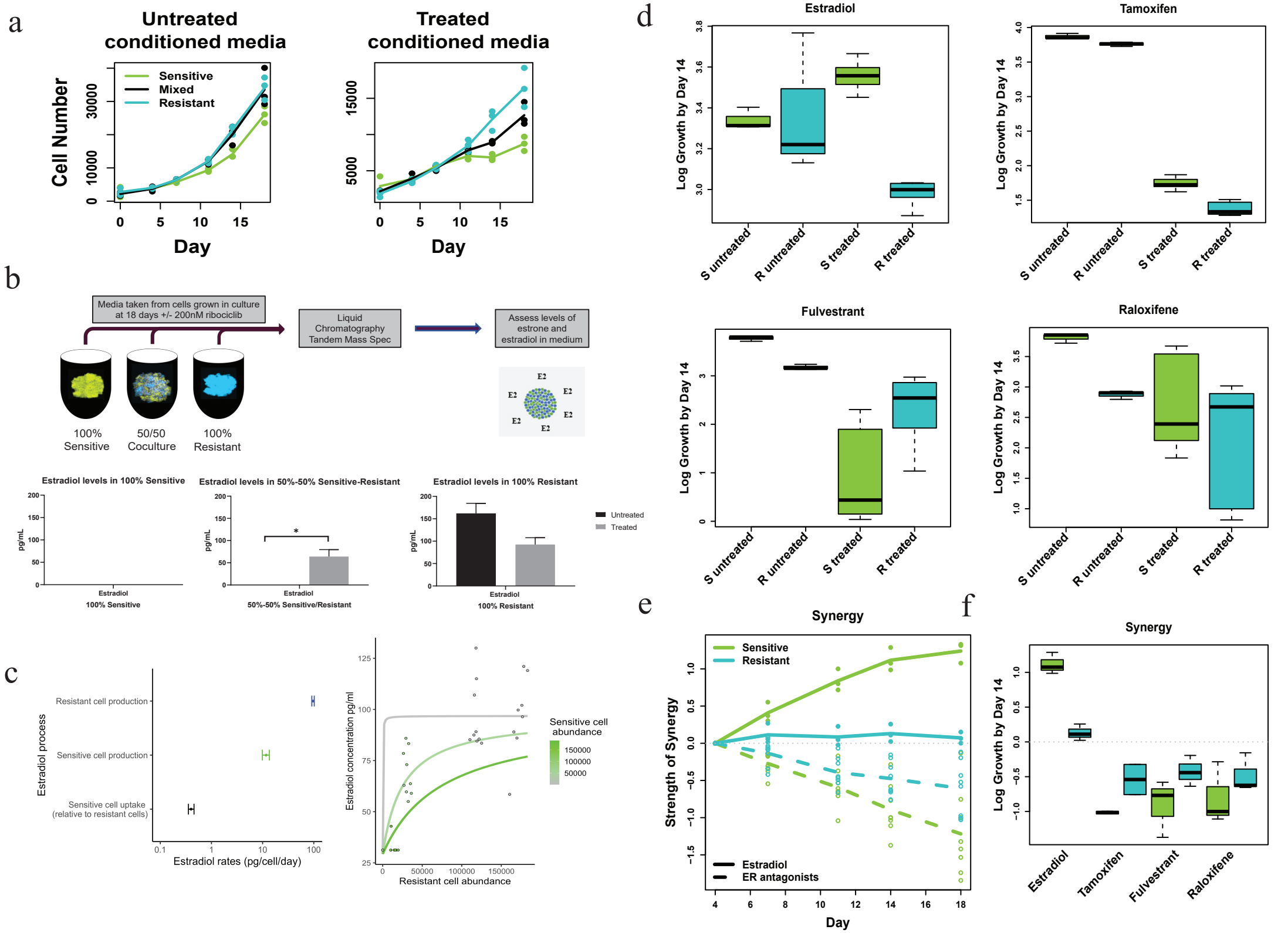

Figure 3. **Underlying biological processes driving facilitation in response to ribociclib treatment. a,** Comparing growth of CAMA-1 spheroids under drug pressure with supplemented conditioned media from spheroids of different compositions. Sensitive and resistant cells were plated by the indicated composition of sensitive and resistant cells in a 3D spheroid format and underwent exposure to untreated or 400nM treated medium to produce conditioned media. 100% sensitive spheroids under drug pressure were then supplemented with different concentrations of conditioned media. Normalized cell counts of sensitive cells supplemented with untreated or treated conditioned media generated from different spheroid compositions. **b,** Liquid chromatography-tandem mass spectrometry (LC-MS/MS) assay for estradiol detection performed on CAMA-1 untreated or ribociclib 400nM treated samples of the following compositions at Day 21: 100% sensitive, 50% sensitive – 50% resistant, 100% resistant samples. **c,** Plots of estradiol production rates of CAMA-1 ribociclib sensitive and resistant cells and sensitive cell uptake of estradiol (relative to resistant cells); estradiol concentration by resistant and sensitive cell abundance **d,** CAMA-1 growth with modifier treatment in monoculture. Box plots of log of growth for sensitive and resistant cells under indicated modifier treatment (estradiol: $p < 0.0001$ for interaction between treatment and cell type indicating reduction in growth of resistant cells and increased growth by sensitive cells, tamoxifen: $p=0.006$ for interaction between treatment and cell type indicating greater reduction in growth of resistant cells, fulvestrant: $p=0.011$ for interaction between treatment and cell type indicating lower reduction in growth of resistant cells , and raloxifene: no significant interaction with growth reduced equally for the two cells types) **e,** CAMA-1 growth with combination treatment in monoculture. Comparison of observed cell growth in combination therapy with that expected under null model that assumes no interaction between the effects of the modifier treatment (estradiol, tamoxifen, fulvestrant, or raloxifene) and ribociclib ($p < 0.0001$ for sensitive cells to grow more rapidly with estradiol and $p=0.0007$ for sensitive cells to grow more slowly with ER antagonist treatment). **f,** Box plots of log of growth for sensitive and resistant cells under modifier treatment estradiol or one of three ER antagonists: tamoxifen, fulvestrant, and raloxifene) and ribociclib ($p < 0.002$ for each ER antagonist to reduce growth of sensitive cells between days 4 and 14 more than resistant cells, but no significant difference among any of the ER antagonists).

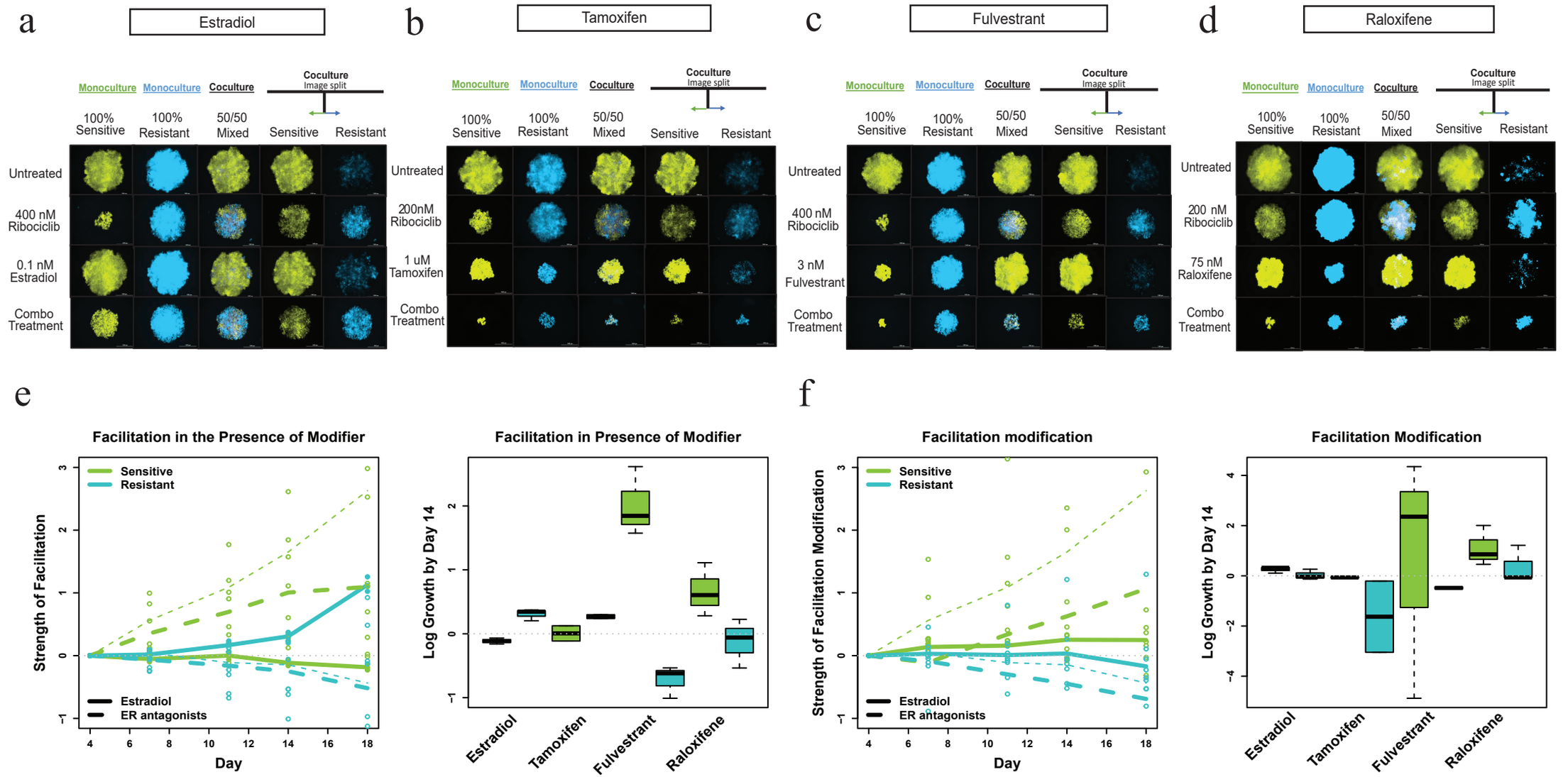

Figure 4. **Modifying endocrine signaling pathways affects spheroid growth and facilitation.** CAMA-1 spheroids of different cell compositions (100% sensitive - green, 50% sensitive- 50% resistant, 100% resistant - blue) cultured in **a,** untreated, 400nM ribociclib, 0.1nM estradiol, or combination 400nM ribociclib with 0.1nM estradiol treated medium for 18 days; images taken on day 18. **b,** untreated, 200nM ribociclib, 1 uM tamoxifen, or combination 200nM ribociclib with 1 uM tamoxifen treated medium for 18 days; Images taken on day 18. **c,** untreated, 400nM ribociclib, 3nM fulvestrant, or combination 400nM ribociclib with 3nM fulvestrant treated medium for 18 days; images taken on day 18. **d,** untreated, 200nM ribociclib, 75 nM raloxifene, or combination 200nM ribociclib with 75 nM raloxifene treated medium for 18 days; images taken on day 18. **e,** Facilitation of CAMA-1 growth in coculture measured as the log of the ratio of the observed cell population to the expectation when treated with modifiers ($p < 0.0001$ for resistant cells to experience greater facilitation than sensitive cells with estradiol, and for sensitive cells to experience greater facilitation than sensitive cells when treated with ER antagonists pooled). The thin dotted lines show facilitation when treated with ribociclib for comparison; Box plots of log of growth for sensitive and resistant cells under treatment (tamoxifen effects not significantly different from estradiol, fulvestrant shows greater facilitation of sensitive cells with $p < 0.0001$ and raloxifene a smaller effect than fulvestrant ($p=0.0035$) but greater from estradiol ($p=0.0052$)). **f,** Facilitation of growth in coculture measured as the log of the ratio of the observed cell population to the expectation when treated with ribociclib in the presence of a modifier ($p=0.007$ for estradiol to reduce facilitation more for resistant cells, no significant effect with the three ER antagonists pooled). The thin dotted lines show facilitation in the absence of the modifier; Box plots of log of growth for sensitive and resistant cells under combination treatments (no significant differences).

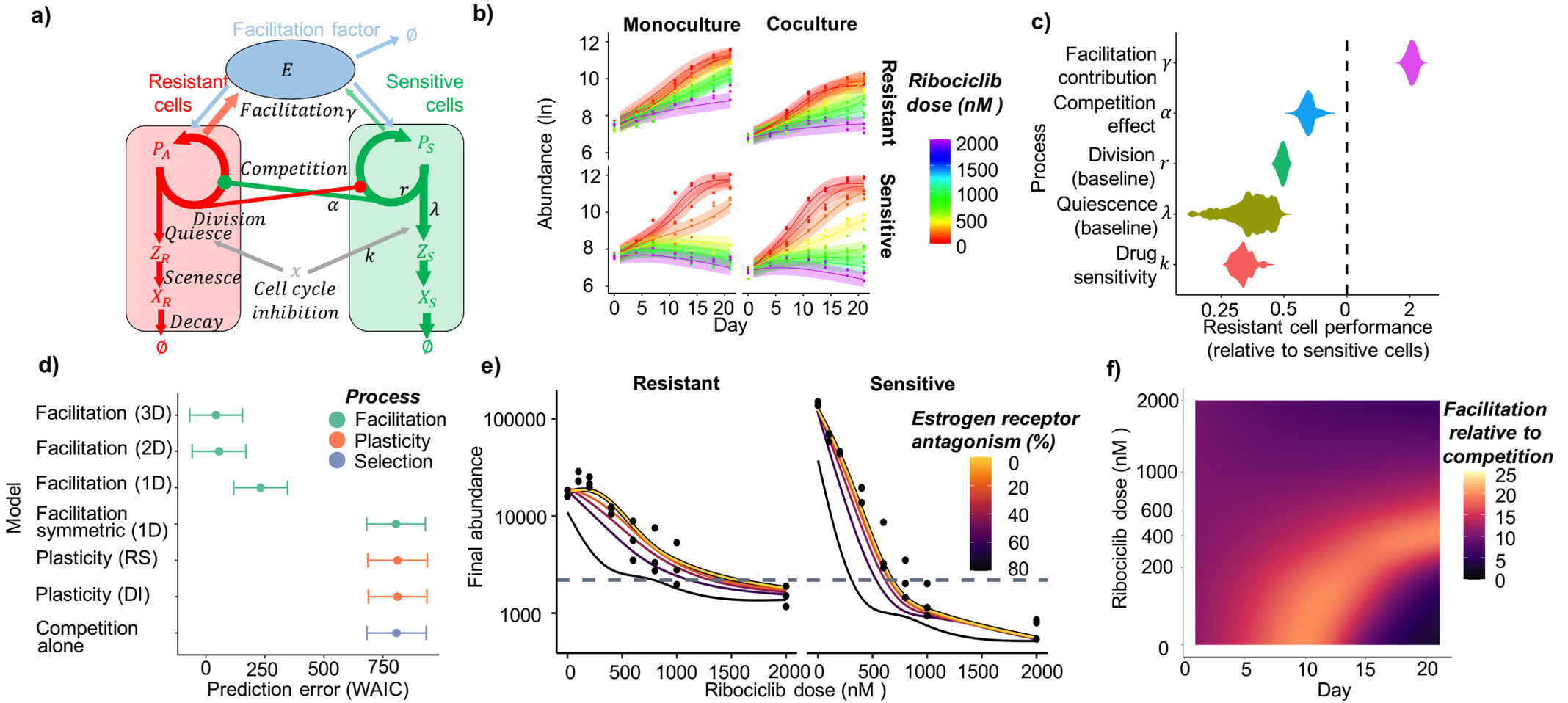

Figure 5. **Measuring the strength and role of facilitation during treatment. a,** Structure of the mechanistic differential equation facilitation model that was fitted to the data. The facilitation model describes the abundance of resistant (red) and sensitive (green) cells which compete (circle headed arrows) and also facilitate one another, through the production of a facilitation factor (estradiol blue) that is used by both cell types to promote cell division. Resistant and sensitive cells transition through proliferative (P), quiescent (Z) and then senescent (X) stages. Cells in the proliferative stage enter the G1/S cell cycle checkpoint at a rate that depends on the abundance of competitors and the concentration of facilitation factors. Upon entry to the G1/S cell cycle checkpoint, cells either divide or enter the quiescent state. Cell cycle inhibitor therapy prevents the accumulation of cell cycle promoting proteins and increases the fraction of cells entering the quiescent stage, rather than dividing. **b,** Prediction of spheroid growth of sensitive and resistant cells (rows), alone or in co-culture (columns) and across a broad range of doses of ribociclib (color). Observed cell counts over time (points) are accurately predicted across all doses and cell type compositions (lines) by the facilitation model and uncertainty in model fits are captured by the 95% high credibility intervals (shaded regions). **c,** Quantification of the resistant and sensitive cells' abilities to facilitate neighboring cell growth, compete for resources, divide or quiesce in the absence of therapy and to respond to the direct impacts of treatment (drug sensitivity). Performance of resistant cells, relative to sensitive cells, is shown for each process (y axis), with the violin plots showing the range of relative performance values which yield predictions of spheroid trajectories consistent with the observed data (shaded region in panel A). Equal performance of the two cell types is signified by the vertical dashed line. **d,** Comparison of the ability of facilitation models (green) to describe the data, relative to models of phenotypic plasticity (red) or competition alone (blue). Low prediction error indicates that the model more accurately explains the spheroid growth data, whilst avoiding overfitting the data by penalizing the model likelihood based on model complexity (using WAIC: widely applicable information criterion). **e,** Prediction of facilitation inhibition on the growth of sensitive and resistant cell coculture populations across drug dose. Data point show the observed final size of replicate spheroids across doses without facilitation blocking (100% facilitation). The thick black bordered lines show the facilitation model predictions of final size. Thinner lines show the predicted reduction in final abundance of resistant and sensitive cells achievable by reducing facilitation (brighter lines indicate greater blocking of facilitation (lower residual facilitation)). **f,** The role of facilitation on spheroid growth, relative to competition, across drug doses. Each point on the surface indicates a specific time and dose. The coloration shows how important facilitation is at that moment (brighter coloration indicates that facilitation is more important). The bright band shows the window of facilitation when abundance of both cell types is increasing but the carrying capacity (maximal density of the spheroid) is not reached.